UNIVERSIDAD DE CHILE
FACULTAD DE CIENCIAS FÍSICAS Y MATEMÁTICAS
DEPARTAMENTO DE INGENIERÍA QUÍMICA, BIOTECNOLOGÍA Y MATERIALES

AN OPERATIONAL RESILIENCE OBJECTIVE TO INTEGRATE IN CAPACITY EXPANSION MODELS FOR GREEN HYDROGEN PRODUCTION THROUGH HRES

TESIS PARA OPTAR AL GRADO DE MAGÍSTER EN CIENCIAS DE LA INGENIERÍA, MENCIÓN QUÍMICA

MEMORIA PARA OPTAR AL TÍTULO DE INGENIERO CIVIL QUÍMICO

ANDRÉS IGNACIO CÁRDENAS OYARZÚN

PROFESOR GUÍA:
Felipe Díaz Alvarado

PROFESORA CO-GUÍA:
Ana Torres Rippa

MIEMBROS DE LA COMISIÓN:
Cristian Salgado Herrera
Juan Asenjo de Leuze de Lancizolle

SANTIAGO DE CHILE
2023

RESUMEN DE LA TESIS PARA OPTAR AL GRADO DE:
MAGISTER EN CIENCIAS DE LA INGENIERÍA, MENCIÓN QUÍMICA
RESUMEN DE LA MEMORIA PARA OPTAR AL TÍTULO DE:
INGENIERO CIVIL QUÍMICO
POR: ANDRÉS IGNACIO CÁRDENAS OYARZÚN
FECHA: 2023
PROF. GUÍA: FELIPE DÍAZ ALVARADO

UN OBJETIVO DE RESILIENCIA OPERACIONAL PARA INTEGRAR EN PROBLEMAS DE EXPANSIÓN DE CAPACIDAD EN PRODUCCIÓN DE HIDRÓGENO VERDE A TRAVÉS DE HRES

El hidrógeno verde (H2V) es un atractivo vector energético producto de su nula emisión de carbono en su proceso de producción y uso, ayudando al sector de transporte y potencia en la transición a energías límpias. El H2V presenta un desafío respecto a resiliencia, ya que su producción depende de energías renovables (ER), las cuales están sujetas a variabilidad.

Chile posee una ventaja para la producción de H2V debido a sus favorables condiciones climáticas, con energía solar y eólica dominantes en el norte y sur del país respectivamente. Se ha desarrollado una estrategia nacional de producción de hidrógeno, la cual contempla convertir a Chile en un productor de H2V a nivel mundial, pero producto del incierto comportamiento de las fuentes de ER, la variabilidad del sistema debe ser abordada, especialmente en redes sin conexión a la red central.

La presente tesis desarrolla una nueva función objectivo de resiliencia operacional para ser incluída en modelos de expansión de capacidad de plantas de H2V. Esta función es construida a partir de las fluctuaciones externas de las fuentes de ER, fallas internas de conversores de corriente, y la capacidad de almacenamiento de masa y energía para otorgar una operación flexible y confiable. La función propuesta captura los detalles de la variabilidad climática en la decisión de instalación de plantas, y compensa la variabilidad del sistema a través de baterías y tanques de hidrógeno.

A través de un caso de estudio en la región del biobío se corrobora el uso de la función objetivo, obteniendo un un diseño de planta más robusto que un modelo puramente económico al mismo precio de equilibrio de hidrógeno, implementando perfiles de expansión que consideran almacenamientos de mayor capacidad. El sistema considera la variabilidad específica de diversas zonas geográficas, implementando capacidad de producción solar y eólica differentes en cada localidad. Comparado el modelo económico, el multi-objetivo reduce la energía eólica en hasta un 51 % producto de su variable naturaleza, compensando con un incremento de las fuentes solares de hasta un 23 % dependiendo de la localidad. El constraste en la capacidad de almacenamiento es notable entre ambos modelos, donde el multi-objetivo presenta un aumento de un orden de magnitud para la capacidad de tanques de hidrógeno y baterías en comparación al modelo económico. En este caso de estudio, los cambios en el diseño requieren una inversión de 0,37 [USD] por kilogramo de hidrógeno producido para lograr un sistema menos variable y más robusto.

RESUMEN DE LA TESIS PARA OPTAR AL GRADO DE:
MAGISTER EN CIENCIAS DE LA INGENIERÍA, MENCIÓN QUÍMICA
RESUMEN DE LA MEMORIA PARA OPTAR AL TÍTULO DE:
INGENIERO CIVIL QUÍMICO
POR: ANDRÉS IGNACIO CÁRDENAS OYARZÚN
FECHA: 2023
PROF. GUÍA: FELIPE DÍAZ ALVARADO

AN OPERATIONAL RESILIENCE OBJECTIVE TO INTEGRATE IN CAPACITY EXPANSION MODELS FOR GREEN HYDROGEN PRODUCTION THROUGH HRES

Green hydrogen is an attractive energy vector due to its zero carbon emission in production and use, supporting transportation and power systems in a transition to cleaner energy worldwide. The production of green hydrogen has a fundamental challenge in resilience since renewable energy (RE) systems are subject to variability.

Chile presents an important advantage for producing green hydrogen due to its favorable weather conditions, with solar and wind energy being dominant in the north and south of the country respectively. The nation has developed a hydrogen strategy that strives to convert Chile into a major global producer of green hydrogen worldwide, but due to the uncertain nature of RE systems, the variability of the energy supply must be dealt with, especially in off-grid systems.

The present thesis develops a novel operational resilience objective function to be included in green hydrogen capacity expansion models. This function is constructed from external source fluctuations, internal converter failures, and the capacity of a dual storage system to provide a more reliable and flexible system. The novel objective functions capture the nuance of variability in the allocation of hydrogen production facilities in different geographical locations and mitigate the expected variability of the system through the storage capacity design in each plant.

An illustrative case study in the Biobío region corroborates the objective function use, obtaining a more robust plant design with the same hydrogen equilibrium price as a purely economic model, implementing higher storage capacities and different expansion profiles that account for storage in a more strategic manner. The systems design also considers the specific variability present in each location, where different wind and solar energy sources capacities are established accordingly. Compared to the economic model, the multi-objective approach reduces the wind power installations by up to 51 % due to their more unstable nature, compensating with the more stable solar source with an increased capacity of up to 23 % depending on the location. The contrast of storage capacities is notable when the proposed objective function is incorporated, resulting in an increase of an order of magnitude in the hydrogen and battery storage capacity. In this case study, the design changes require an investment of $0.37 [USD] per kilogram of produced hydrogen to achieve a less variable and more robust system.

La medicina, leyes, administración, ingenierías son muy nobles y necesarias para sostener la vida, pero la poesía, belleza, romance, amor... Es por eso que vivimos

Sociedad de los Poetas Muertos

Agradecimientos

Agradezco infinitamente a mi familia, a mis padres, Jorge, Kattia, quienes desde pequeño me enseñaron el valor del esfuerzo, el conocimiento y el trabajo. Quienes siempre me apoyaron, me amaron, me cuidaron y educaron. Me siento afortunado y profundamente agradecido de poder decir que ustedes dos son mis padres. Quiero agradecer a mi hermano y mis hermanas, Marcos, Debora, Bárbara, gracias por siempre estar ahí. Gracias por darme la posibilidad de tener hermanos a los que siempre puedo recurrir para cualquier cosa, y de los cuales estoy orgulloso a más no poder.

A mis amigas y amigos de la universidad, Camilo, Blanca, Mati, Cid, Basadita, Pancho, Javo, Mery, Mamanda, gracias por todo el apoyo, las risas, los carretes y la buena amistad que me dieron. Muchas gracias a ti también, Almendra, gracias por acompañarme durante tantos años, y ayudarme a lograr ser el hombre que soy hoy. A mis amigos de la vida, Tomás, Luciano, gracias por ser un hombro en el cual reír y llorar. Claudia, gracias por estar aquí, gracias por tu ternura y tu bella compañia en los últimos momentos de este escrito. Gracias a los cabros, a los que siempre han estado y siempre estarán, no alcanzo a mencionarlos a todos pero ustedes saben quiénes son. No podría soñar con tener mejores amigos que todos ustedes, y no me alcanzan las palabras para todo lo que les quiero agradecer.

Muchas gracias a todas y todos los profesores que dentro de la universidad han forjado mi forma de pensar, de aprender, de enseñar y de ver la vida. Mil gracias a ti, Felipe, gracias por la mentoria y la tremenda capacidad de encaminarme a mis propios intereses. Muchas gracias por la confianza y el apoyo en todo este tiempo. Muchas gracias Ana, por confiar en este proyecto y darme la oportunidad de trabajar contigo.

Gracias a mis profesores de composición, Sebastián, Andrés, muchas gracias por acompañarme y guiarme en el camino de mi propio arte. Por apoyarme en no rendirme a la idea de que uno es una sola cosa, solo un ingeniero, solo un estudiante. Nunca dejaré de vivir la música como ustedes dos me lo enseñaron, sin importar quién piense lo contrario. Pablo, gracias por ayudarme en el gran paso de dejar los males del pasado atrás. Gracias por sanar mi cuerpo y alma a través del arte que hoy llevo orgullasamente conmigo a todos lados.

Agradezco también a todos esos desconocidos, a quienes uno nunca contempla, los que trabajan día a día en crear y mantener una sociedad donde podemos realizarnos como persona. El resultado que hoy presento es fruto de mi esfuerzo, sin duda, pero es también el resultado del esfuerzo y trabajo de muchos héroes anónimos gracias a los cuales puedo ser hoy quien redacta este escrito. A todos ustedes, muchas gracias.

TABLE OF CONTENT

1. Introduction **1**
1.1. Renewable energy systems . . . 1
1.2. HRES modelling literature review . . . 1
1.2.1. Classical optimization techniques . . . 2
1.2.2. Metaheuristics . . . 2
1.2.3. Hybrid methods . . . 3
1.3. Resilience in power systems . . . 3
1.4. Aim of this study . . . 4

2. Problem statement **6**
2.1. System modelling . . . 7
2.1.1. Problem super-structure . . . 7
2.1.2. Representative days approach . . . 8
2.1.3. Generation models . . . 8
2.1.4. Battery storage . . . 8
2.1.5. Alkaline electrolysis model . . . 9
2.1.6. Hydrogen Compressor . . . 9
2.1.7. Hydrogen tank storage . . . 10
2.1.8. Capacity expansion modelling . . . 10
2.2. Economic objective function . . . 11
2.2.1. Terrain investment . . . 11
2.2.2. CAPEX . . . 11
2.2.3. OPEX . . . 12
2.2.4. H2 storage opportunity cost . . . 12
2.2.5. Discount factor . . . 12
2.3. Objective function development . . . 13
2.3.1. Resilience in this context . . . 13
2.3.2. Indicator constituents . . . 13
2.3.3. External variability . . . 13
2.3.4. Internal variability . . . 14
2.3.5. Proposed objective . . . 15

3. Case study **16**
3.1. Locations and climate data . . . 16
3.2. Projected demand . . . 17
3.3. Results . . . 17
3.3.1. Computation time . . . 17

3.3.2. Solution multiplicity 17
3.3.3. Pareto front and equilibrium prices 18
3.3.4. Capacity expansion: single and multi objective comparison 19
3.3.5. The role of storage: Single and multi objective comparison 21
3.3.6. Results remarks 22

4. Conclusion **25**
4.1. Summary of the Thesis and Key Contributions 25
4.2. Future Recommendations 25

BIBLIOGRAPHY **26**

ANNEXES **32**
A. Alternative designs 32
B. Hydrogen demand projection 33
C. Electrolysis technologies cost comparison 33
D. Condensed model formulation and nomenclature 35
E. Parameter values 40

List of Tables

3.1. Optimal value for the objective functions in each single-objective model. Alternate solutions' values are presented as a difference from the optimal solution objective. 17

3.2. Results overview for the economic and MO models. Capacities are presented as intervals of the minimal and maximum values in the time horizon, expresses as [Min - Max]. 23

B.1. Parameters for the demand projection through a learning curve behavior. . . . 33

E.1. Parameters for the case study 40

List of Figures

2.1. Graphical representation of the regional production problem. 6
2.2. Superstructure for a generic solar/wind green hydrogen production plant. Solar and wind generators can supply power directly to the electrolyzer and compressor; a battery system can be placed to balance the intermittencies of the generators. The demand for hydrogen can be directly satisfied from production or from intermediate storage tanks. 7
2.3. Architecture of the hydrogen production plant with relevant converters. 14
3.1. Averages climate statistics of solar radiation (a) and wind speed (b) for each location at each trimester. (Own elaboration with the data provided by the wind and solar explorers [56, 57]) 16
3.2. Hydrogen equilibrium price for each Pareto point. 18
3.3. Expansion profiles of the economic model for Negrete (a) and Aguapie (b) respectively. 19
3.4. Expansion profiles of the heteronomy model for Negrete (a) and Aguapie (b) respectively. 20
3.5. Expansion profiles of the multi objective model for Negrete (a) and Aguapie (b) respectively. 20
3.6. Mass storage per location profile for the single and multi objective models. . . 21
3.7. Heteronomy objective function behavior. 22
3.8. Equilibrium price of hydrogen in each Pareto optimal solution. 24
A.1. Alternative designs for the Aguapie expansion. Obtained through the "No good" integer cut. 32
B.1. Global hydrogen demand projection through a learning curve for pessimistic, normal and optimistic scenarios. 34

Chapter 1

Introduction

1.1. Renewable energy systems

Fossil fuels and their greenhouse gas emissions have considerably impacted the environment, specifically on climate change [1]. Renewable energies (REs) are proposed to mitigate this problem; however, REs present technical challenges in contrast to fossil resources. Renewable sources are susceptible to exogenous effects such as weather conditions, and in some RE systems, the offer of primary energy is not predictable (e.g., tidal and wind energy). As a consequence, the supply has to deal with uncertainty [2].

The Hybrid Renewable Energy System (HRES) is a methodology developed to withstand this deficiency. This proposes that a system composed of coupled RE sources can complement each other's deficiencies and produce a more stable energy output. In addition, these systems consider various types of energy storage technologies to further improve the stability [3].

Green hydrogen has been studied extensively as an energy carrier with no direct carbon emissions at the production phase [4]. This attractive property has led to international interest in developing hydrogen production based on hybrid renewable energy systems. Mainly, Chile is known as one of the countries with a significant capacity to produce clean energy, specifically from solar and wind sources, and has the opportunity to become a global leader in green hydrogen production [5].

However, dealing with the variability of RE sources is still a pending question in the design phase of regional or national-scale HRES. There is a lack of resilience metrics integration at the design phase of long-term energy systems [6]. This paper provides a quantitative approach to HRES resilience by considering the resource variability and the intrinsic failure rate of physical components in the system. This quantitative approach is expressed as an objective function in a MILP model to decide the capacity expansion of regional-scale HRES.

1.2. HRES modelling literature review

Mathematical programming in HRES design is used to achieve a specified goal (such as minimal cost or emissions) while considering pertinent constraints associated with the system and its parts [7]. Different optimization techniques, such as classical techniques, metaheuristics, and hybrid methods, can be employed to find optimal solutions successfully.

1.2.1. Classical optimization techniques

Linear programming approaches to HRES design have been applied extensively. Nonetheless, linear formulations cannot accurately represent the complexities of HRES systems, such as non-linear physical constraints or binary choices of expansion or investment.

Considering logical decisions and integer values, mixed integer programming has been implemented to assess for more realistic models. Ferrer-Martí et al. (2013) demonstrated the performance of an integer based model to determine size an locations of an HRES design, based on the minimization of the investment cost [8]; Ahadi et al. (2016) developed a novel approach for optimal wind/PV and battery storage islanded system design, considering the range of battery storage dependent on the capacity of the sources to satisfy a fixed demand [9]; Lara et al. (2018) proposed a deterministic multi-scale formulation for electric power infrastructure planning, considering annual generation, investment and hourly operational decisions [10]; Yu et al. (2019) studied the design and operation of HRES through a two-stage stochastic MILP model, resulting in a lower total cost than deterministic models [11]; Alberizzi et al. (2020) developed a model that considers type of energy generation, optimal number of equipment's, storage technologies and optimal management strategies, to minimize the systems dependence on fossil fuels while supplying a fixed demand for a case study [12]; Vera (2020) proposed a resilience indicator based on the health overtime curve of a power system, and analyzed its effectiveness through an integer programming approach [13]; Pan et al. (2020) developed a bi-level mixed-integer model to improve the systems economy and minimize the levelized cost of hydrogen with the use of solar, wind and geothermal sources [14]; Lim et al. (2021) modelled the transition of localized HRES produced energy to hydrogen and other potential carriers. The authors developed a MILP in a P-graph superstructure setting, considering a petrochemical industrial complex in South Korea as the case study [15]; Weimann et al. (2021) studied hydrogen production through HRES considering dual storage technologies. Through a MILP approach, a zero-emissions wind-dominated system was developed, and how hydrogen demand affects the use of it as storage instead of as a commodity [16]; Corengia et al. (2022) formulated a model that considers the selection of energy sources, type of electrolyzer, its capacity and energy storage devices, concluding that hydrogen has a prospect that outreaches energy surplus storage only [17]; Li et al. (2022) proposed simplifications for MILP models of generation and transmission expansion planning of power systems [18].

Implementing nonlinear programming (NLP) and mixed integer nonlinear programming (MINLP) methods is less abundant than other classical optimization techniques. El-Zeftawy et al. (1991) determined a cost-effective optimal configuration for a wind-diesel and wind-battery hybrid for the seasons of the year; Ashok (2007) discussed different system components and solved an NLP formulation to attain minimal life cycle cost for a typical rural community [19]; Obaro et al. (2018) developed and optimal control and management system for hybrid energy systems through an MINLP objective function. The proposed system significantly minimizes the cost and improves the supply reliability compared to a single system [20]; Gutiérrez et al. (2022) determined the optimal PV solar kit grid-connected sizing with battery storage that minimizes the average energy cost in a finite time horizon [21].

1.2.2. Metaheuristics

Metaheuristic search techniques are nature-inspired algorithms that achieve optimal solutions to optimization problems [22]. Some examples are genetic algorithms (GA), particle

swarm optimization (PSO), and ant colony (AC) algorithms.

Lee et al. (2009) proposed a multi-pass dynamic programming to determine the optimal size of a battery energy storage system and contact capacities of customers at the Taiwan Power Company [23]; Hakimi et al. (2009) proposed two hybrid system configurations contemplating fuel cells, wind units, an electrolyzer, a reformer, a compressor, an anaerobic reactor, and a hydrogen tank, and applied a PSO method to determine the sizing of the system under a fixed demand [24]; Koutroulis et al. (2010) implemented genetic algorithms on an HRES design model consisting of PV and wind energy for water desalinization energy supply, effectively supplying water demand and minimizing economical cost [25]; Zhao et al. (2013) optimized an HRES design on a recently developed standalone microgrid on Dongfushan, maximizing the useful life of lead-acid batteries and minimizing power generation cost via the nondominated sorting genetic algorithm NSGA-II [26]. The results show how the proposed solving method can effectively optimize the systems operations in different scenarios; Fetanat et al. (2015) applied an ant colony optimization on an HRES sizing problem consisting of PV and wind energy systems. The mathematical model considered continuous and integer variables, and minimizing the total cost of the system considering maintenance [27]; González et al. (2015) used a genetic algorithm to design a minimal cost HRES to supply a fixed electrical demand, and through a sensitivity analysis determined that the systems optimal solution design was economically robust [28].

1.2.3. Hybrid methods

Combining two or more optimization techniques can overcome the limitations of the individual techniques. This combination is referred to as hybrid methods [22].

Katsigiannis et al. (2012) proposed and hybrid simulated annealing (SA) and tabu search (TS) hybrid algorithm for the solution of sizing a small autonomous power system, improving the convergence and quality of the solution to each algorithm separately [29]; Khatib et al. (2012) solved an optimization problem for hybrid PV/wind system based on loss of load probability (LLP) and system cost through a hybrid iterative/genetic algorithm [30]; Sinha et al. (2015) reviewed recent trends in HRES optimization techniques, and stated that hybrid techniques of two or more algorithms could overcome limitations of the traditional single optimization methods [31]; Wang et al. (2015) developed a receding horizon strategy to account for demand response and operational optimization of an HRES while considering real-time predictions and a demand-responsive scheme. The effectiveness of the strategy is analyzed through a residential case study [32]; Kavadias et al. (2018) created an algorithm to asses for hydrogen-based storage system in an autonomous electrical network, providing optimal sizing of the hydrogen storage system to maximize the recovered energy that would otherwise be curtailed [33].

1.3. Resilience in power systems

Resilience can be understood as the capacity to withstand misfortune and recover from undesirable events. Applied to any specific fields such as energy systems, infrastructure, material science, and others; this definition needs to be more specific in order to propose a resilience indicator. This specificity depends on the studied system. The most common approach to define resilience in an energy system is through the systems *health-overtime-curve*, representing the transient state of specific properties over time after an incident that

disrupts a stable state. As exposed by Gasser et al. [34], a multiplicity of resilience definitions and measures are defined through this curve. They are clustered in two groups: *draw-down*, which represents the system's loss due to an undesired event, and *draw-up*, as the system's ability to recover from said adverse event. Some examples of the draw-down section of the curve are:

- **Robustness:** referring to a system's capacity to withstand a given level of stress or demand without any loss of function [35].
- **Absorptive:** as the degree to which a system can absorb the impacts of a perturbation and minimize consequences with minimal effort [36].
- **Resist:** referring to the capacity of the system to stay within acceptable ranges of functionality after a negative event [37].

The draw-up section is associated with recovery behaviors. Some examples are:

- **Recover:** capacity to recover quickly and at low cost from potentially disruptive events [37, 38].
- **Adapt:** how the system adapts to the newly introduced conditions [39].
- **Rebuild:** capacity to rebuild all the functions and establish normalcy [40].

Vera [13] studied the resilience of an HRES design through a novel resilience indicator and its solution employing MILP optimization. Resilience is considered a system's capacity to recover from catastrophic events, such as earthquakes, and conducted a comprehensive review of resilience indicators based on the system health over time curve. This approach is innovative in considering resilience as an objective function in HRES design. Nonetheless, the multiplicity of ways one can define resilience means that the author's approach does not encompass some important nuances, such as energy supply stability in normal conditions.

Cho et al. [41] reflect on the simultaneous consideration of reliability (withstanding component failure), flexibility (achieving feasible operation under uncertain conditions), and resilience (capacity to withstand catastrophic events) in power systems planning as a necessity for future advanced optimization, defining and differentiating this three terms and their applications.

1.4. Aim of this study

Most of the studied resilience metrics in section 1.3 are based on the system's *health-over-time* curve. Because of this, resilience metrics can be used in dynamic models for planning energy systems. Consequently, the proposed indicators require information on how much system loss occurred at a specific time, how much it lasted, and how fast the system dropped quality and recovered functionality. When design considers long-term planning, such as capacity expansion models, it is not possible to assess with confidence what disruptive events will occur and their magnitude. According to Hammer and Veith [6], a research gap exists in optimizing HRES with respect to robustness and resilience. Because of this, an alternative indicator to measure resilience is needed for a yearly planning model.

The novelty of this paper is a multidimensional design of a regional green hydrogen production system through a novel objective function for HRES operational resilience. Accounting for the primary power sources variability, the internal physical components failure rate, and the mitigation through a dual storage system of batteries and H_2 storage tanks. The trade-off between an increased storage capacity, renewable energy variability, plant allocation, and the cost of the system is analyzed through a multi objective optimization of present cost and the proposed operational resilience function through a regional capacity expansion case study in Chile.

Chapter 2

Problem statement

This work focuses on the allocation and capacity expansion of off-grid green hydrogen production facilities within a delimited geographical region subject to a given hydrogen demand. Each location in the region needs to define whether or not to install renewable energy (RE, solar, or wind) generators, a bank of batteries to store that energy, an electrolyzer, the associated hydrogen compression stage, and tanks for storage. In addition, it's required that these designs be resilient. Figure 2.1 depicts a representation of the problem.

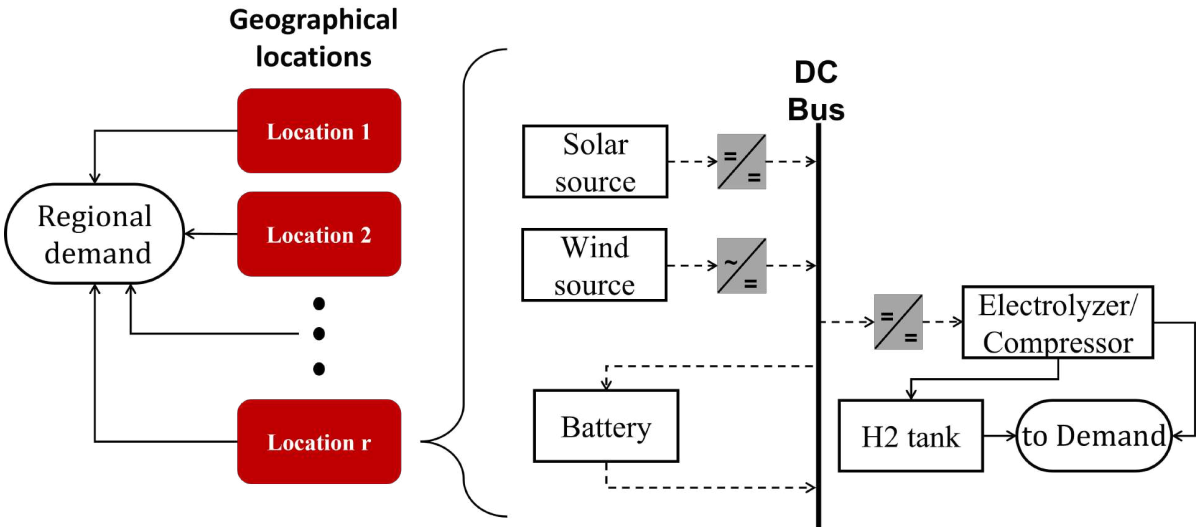

Figure 2.1: Graphical representation of the regional production problem.

Due to the intermittency of the RE sources, variability in the energy output is expected. Said variability may result in a hydrogen production deficit if the system cannot overcome the energy shortfall. Storage capacity, either in batteries or in hydrogen tanks, provides the system with flexibility in operation, reducing the effects of an energy deficit but incurring a trade-off of higher capital and operational cost. The main objective of the allocation and subsequent capacity expansion is to determine the optimal sizing and investment plan for each location each year, thriving for an economical and flexible regional hydrogen production system.

2.1. System modelling

The proposed model is a Mixed Integer Linear Programming superstructure-based problem, and in the following subsections, a summary of the model will be stated. The model is composed of r locations in the considered geographical region, d representative days hourly discretized by the index t. A complete formulation is available at Appendix D. A MILP approach is considered over LP or MINLP for this problem to provide sufficient mathematical tools to model decisions of investment and design while maintaining a trackable computation time.

2.1.1. Problem super-structure

The superstructure of the problem is a simplified representation of a solar/wind green hydrogen production plant with integrated energy and mass storage. Since the model does not encompass interactions between each plant, a process diagram for a generic plant can be defined for each location. This is shown in Figure 2.2, where mass and energy flows are presented as dashed and filled arrow lines along with equipment capacity variables as bold text. Each piece of equipment can vary its capacity in the time horizon according to the constraints presented in section 2.1.8. The nomenclature associated with the model superstructure is presented in Annex D.

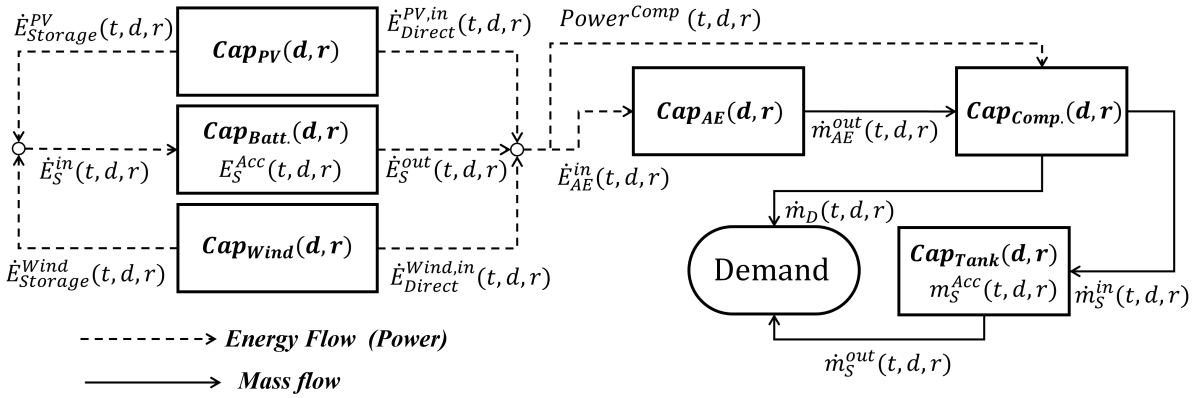

Figure 2.2: Superstructure for a generic solar/wind green hydrogen production plant. Solar and wind generators can supply power directly to the electrolyzer and compressor; a battery system can be placed to balance the intermittencies of the generators. The demand for hydrogen can be directly satisfied from production or from intermediate storage tanks.

The superstructure contemplates that renewable sources can directly supply the electrolyzer with power for hydrogen production or feed a battery system to store energy. The battery system can also accumulate energy and discharge power to the electrolyzer. Only Alkaline electrolysis is considered in this study since, at the present date, it is the most cost/efficient technology at the moment (see Annex C). The electrolyzer supplies a compressor that raises hydrogen pressure to 300 [Bar] for subsequent storage at high-pressure tanks or its departure for demand. The high-pressure tank can also discharge to supply demand when needed. In this case, no transportation methods for the demanded hydrogen are analyzed since it falls outside the studies battery limit.

2.1.2. Representative days approach

Capacity expansion of power systems based entirely on renewable energy faces several complications when trying to capture all the nuances and details of climatic conditions for a rigorous plant design, mainly when relying on historical data to make future predictions. Furthermore, modeling hourly operations of said systems through a decade-long time horizon would turn the optimization of the system into a problem that might be untractable [42]. To withstand this complication, a representative days approach is considered for the case study. This method is based on selecting specific periods of a historical year; each period is then represented by a characteristic day, which encompasses the overall behavior of the property being analyzed [43]. In this case, said properties are solar radiation and wind speed.

The time horizon of this study will span 15 years, from 2025 to 2040 where each year is subdivided into three representative days, grouping January to April, May to August, and September to December. Each day presents an hourly subdivision of time, from 1 to 24 hours. It is important to note that since the scope of this publication aims to develop an objective function for resilience, more rigorous methods to evaluate climatic conditions and the statistical analysis of such for the selection of representative days are not considered. Furthermore, no forecast prediction of how climatic conditions will vary due to natural or anthropocentric causes are implemented for the same reason.

2.1.3. Generation models

Renewable energy sources are modeled according to the installed equipment area in each location on a corresponding representative day. The variables associated with the installed PV panel area and wind turbine swipe area are $A^{PV}_{d,r}$ and $A^{Wind}_{d,r}$. The generation model for solar energy is presented in equation 2.1, where power is dependent on installed area, solar radiation, and panel efficiency as a linear equation [44].

$$\dot{E}^{Direct}_{PV,t,d,r} + \dot{E}^{Storage}_{PV,t,d,r} = \eta_{PV} \cdot {A^{PV}}_{d,r} \cdot {G^{Sun}}_{t,d,r} \tag{2.1}$$

The generation model for wind turbines is developed through an energy balance, where the total power output of the turbine is dependent on the installed swipe area, the turbine's capacity factor, average wind speed, and air density [45]. Equation 2.2 presents the generation model for wind turbines. In this study, the height of the turbines is assumed to be 80 [m] since the in-depth design of equipment is not considered in the scope of the research.

$$\dot{E}^{Direct}_{Wind,t,d,r} + \dot{E}^{Storage}_{Wind,t,d,r} = \frac{1}{2} \cdot C^{Wind}_{p} \cdot A^{Wind}_{d,r} \cdot \rho_{Air} \cdot (v^{Wind}_{t,d,r})^3 \tag{2.2}$$

A specific factor is extracted from the literature to relate the swipe area with the used terrain. Afsharian et al. [46] provides a systematic approach to determine said factor based on a previously developed method [47], and in this study, its value is set to $1.7 \cdot 10^{-3}$ $\left[\frac{m^2 \text{ swipe}}{m^2 \text{ terrain}}\right]$.

2.1.4. Battery storage

Battery systems present two relevant modeling requirements, the energy balance that contemplate inputs, outputs, and accumulated energy and the minimal and maximal states of charge (SOC) required to preserve the battery system's correct operation and lifetime. The energy balance of the battery system is presented in equation 2.3, where charge, discharge, and passive losses are considered.

$$Es^{Acc}{}_{t,d,r} = \left[1 - L^{Battery}\right] \cdot Es^{Acc}{}_{t-1,d,r} + \Delta t \cdot \left(\eta_{Charge} \cdot \dot{E}s^{in}_{t-1,d,r} - \frac{\dot{E}s^{out}_{t-1,d,r}}{\eta_{Discharge}}\right) \tag{2.3}$$

To equate for a linear constraint for the battery systems SOC nominal battery capacity constraints the stored energy according to the minimal and maximal SOC presented in equation 2.4.

$$SOC_{min} \cdot Cap_{Battery,d,r} \leq E^{Acc}_{t,d,r} \leq SOC_{max} \cdot Cap_{Battery,d,r} \tag{2.4}$$

2.1.5. Alkaline electrolysis model

Water electrolysis is the chemical reaction used to produce hydrogen from renewable energy sources. The hydrogen production is considered to be linearly dependent on the supplied power to the electrolyzer according to equation 2.5.

$$\dot{E}^{in}_{AEt,d,r} = \frac{\dot{m}^{out}_{AEt,d,r} \cdot \Delta H}{\eta_{AE}} \tag{2.5}$$

Where η_{AE} and ΔH are the electrolyzer's power to hydrogen efficiency and the reaction enthalpy respectively. The $\frac{\Delta H}{\eta_{AE}}$ factor is equal to 57.3 kWh/kg for the alkaline electrolysis [48, 49].

An essential characteristic of AE technologies is that at small/medium capacities, a minimum load factor is required to avoid persistent shutdown periods in the electrolyzer operation, which can be incorporated through binary variables in a mixed integer programming approach [17]. However, since this study deals with large-scale hydrogen production, the number of required stacks is sufficient to render the minimum load factor negligible, denying the need for more binary variables and a more complex model formulation.

2.1.6. Hydrogen Compressor

The compression stage for hydrogen can be considered as a classical polytropic compression according to Martin et al. [50]. Equation 2.6 characterizes the power consumption for hydrogen compression.

$$P^{Comp} = \frac{\dot{m}^{in}_{Comp} \cdot RkT}{MW \cdot (k-1) \cdot \eta_{Comp}} \left(\left(\frac{P_{H_2}}{P_{el}}\right)^{\frac{k-1}{k}} - 1\right) \tag{2.6}$$

Where the compressors power requirement is dependent on the hydrogen mass flow ($\dot{m}^{in}_{Comp}$), the compressor efficiency (η_{Comp}), the polytropic coefficient (k), the molecular weight of hydrogen (MW), and the ratio of out/in pressure ($\frac{P_{H_2}}{P_{el}}$) inside the vessel.

To represent the compression model in a linear setting, the pressure inside the vessel is considered constant and equal to the maximum pressure of the vessel. This consideration allows a linear representation of the compression model, shown in equation 2.7.

$$Power^{Comp}_{t,d,r} = k_{Compressor} \cdot \dot{m}^{out}_{AEt,d,r} \tag{2.7}$$

Where k encompasses the constant values of parameters in equation 2.6 and is set to 4 $[\frac{kWh}{kg\ H_2}]$ according to Corengia and Torres [17].

2.1.7. Hydrogen tank storage

Analogous to battery storage, hydrogen storage presents two crucial considerations, mass balance for the storage system and maximal hydrogen level (HL) as a security factor. Equation 2.8 presents the mass balance associated with the pressurized tank system hourly, where a discharge efficiency of 95 % is applied to account for pumping or leakage losses [51].

$$ms^{Acc}{}_{t,d,r} = ms^{Acc}{}_{t-1,d,r} + \Delta t \cdot \left(\dot{m}s^{in}_{t-1,d,r} - \frac{\dot{m}s^{out}_{t-1,d,r}}{\eta_{Tank}} \right) \tag{2.8}$$

As a safety measure, the maximum hydrogen level for the pressurized tank is considered as 95 % of the nominal capacity. Equation 2.9 presents the constraint for the stored hydrogen mass.

$$0 \leq ms^{Acc}{}_{t,d,r} \leq HTL_{max} \cdot Cap_{Tank,d,r} \tag{2.9}$$

2.1.8. Capacity expansion modelling

Each technology from any location can augment or diminish its capacity within certain restrictions. It is considered that any expansion project, no matter its magnitude, requires a year-long development, and the augmentation of the capacity becomes available gradually at each trimester. A decrease in technology is considered to take one trimester of the year. Equation 2.10 presents the characterization of a technology capacity through the time horizon as a stock constraint. As a safety measure, the maximum hydrogen level for the pressurized tank is considered as 95 % of the nominal capacity. Equation 2.9 presents the constraint for the stored hydrogen mass.

$$Cap_{i,d,r} = Cap_{i,d-1,r} + \sum_{\hat{d}=d}^{d+2} \left(\frac{1}{3} CapE_{i,\hat{d}} \right) - CapD_{i,d-2,r} \tag{2.10}$$

Where $\sum_{\hat{d}=d}^{d+2} \left(\frac{1}{3} CapE_{i,\hat{d}} \right)$ corresponds to the gradual augmentation of capacity by trimesters.

The system's expansion and decrease are associated with binary variables, defined in equations 2.11 and 2.12 respectively.

$$Y_{i,r,d} = \begin{cases} 1 & i \text{ starts an expansion at day } d \text{ in location } r \\ 0 & \neg \end{cases} \tag{2.11}$$

$$X_{i,r,d} = \begin{cases} 1 & i \text{ starts a downgrade at day } d \text{ in location } r \\ 0 & \neg \end{cases} \tag{2.12}$$

With the binary variables for increase and decrease projects, logical relations arise. If an expansion project is being developed for a technology at a specific location, no other expansion or decrease project can be started for said technology at that location. This is presented in equation 2.13, where no simultaneous expansion and downgrade is allowed; equation 2.14, which states that while an expansion project is being developed, no subsequent expansions can be started; and equation 2.15, where no decrease project is allowed while an expansion is taking place.

$$Y_{i,d,r} + X_{i,d,r} \leq 1 \tag{2.13}$$

$$\sum_{\hat{d}=d+1}^{d+2} Y_{i,\hat{d},r} \leq 2 \cdot (1 - Y_{i,d,r}) \tag{2.14}$$

$$\sum_{\hat{d}=d+1}^{d+2} X_{i,\hat{d},r} \leq 2 \cdot (1 - Y_{i,d,r}) \tag{2.15}$$

Big-M constraints are implemented to associate the existence of capacity-altering projects with the corresponding magnitude of the capacity augmentation/decrease. Equations 2.16 and 2.17 show said constraints.

$$CapE_{i,d,r} \leq M \cdot Y_{i,d,r} \tag{2.16}$$

$$CapD_{i,d,r} \leq M \cdot X_{i,d,r} \tag{2.17}$$

Annex E exhibits the selected values for the **M** parameter at each Big-M constraint.

2.2. Economic objective function

The economic objective function is presented in equation 2.18. Terrain acquisition, CAPEX, OPEX, H2 opportunity cost, and a discount factor are considered to account for the system's economy and not only for its monetary cost.

$$\text{Min: } Terrain + \sum_{d \in D} DF_d \cdot (CAPEX_d + OPEX_d + {C^{H_2}}_{Op_d}) \tag{2.18}$$

The subsequent subsections present the definition of the terms implemented in the economic function and its corresponding equations.

2.2.1. Terrain investment

According to the SII database, each location has its own cost and available area [52]. The terrain is acquired the first year for each location, and the total cost is linearly dependent on the bought area as stated in equation 2.19.

$$Terrain = \sum_{r \in R} {C_r}^{Area} \cdot A_r \tag{2.19}$$

2.2.2. CAPEX

CAPEX considers the installation cost of a certain capacity for a specific technology. Equation 2.20 presents the implementation cost at the beginning of the time horizon, where the installed capacity of day 0 is related to implementation cost. Meanwhile, equation 2.21 defines the cost of subsequent capacity expansion, where the implementation cost is related to the expansion of capacity, not to the current installed capacity at said representative day.

$$CAPEX_0 = \sum_{i \in I,\, r \in R} {C_i}^{Impl} \cdot Cap_{i,0,r} \tag{2.20}$$

$$CAPEX_{d \neq 0} = \sum_{i \in I,\, r \in R} {C_i}^{Impl} \cdot CapE_{i,d,r} \tag{2.21}$$

2.2.3. OPEX

OPEX is defined as operational and maintenance cost (O&M) and is considered a percentage of installed capacity. Equation 2.22 exhibits the OPEX associated with a particular representative day.

$$OPEX_d = \sum_{i \in I,\, r \in R} {C_i}^{Op} \cdot {C_i}^{Impl} \cdot Cap_{i,d,r} \tag{2.22}$$

The parameter ${C_i}^{Op}$ corresponds to the O&M costs of each trimester associated with the installed capacity.

2.2.4. H2 storage opportunity cost

In this study, an opportunity cost for stored hydrogen is considered. Since the supplied demand is less than the overall national/international demand, the stored hydrogen is in direct capacity to be sold. However, if used as storage, a potential economic gain is lost. Equation 2.23 shows the stored H2 opportunity cost directly related to stored H2 mass.

$${C_{H_2}}^{Op}{}_d = {P_{H_2}}^{Sale} \sum_{t \in T,\, r \in R} {ms^{Acc}}_{t,d,r} \tag{2.23}$$

It is important to note that stored energy does not have an opportunity cost. Since the proposed plants present off-grid power systems, it is not possible to directly sell the stored energy, hence not providing any opportunity cost for storage.

2.2.5. Discount factor

A discount factor is considered for the CAPEX, OPEX, and H2 opportunity cost to account for the time value of money. Equation 2.24 exhibits the discount factor for an interest rate r.

$$DF_d = \frac{1}{(1+r)^d} \tag{2.24}$$

To account for end-of-time effects, the discount factor of the last representative day is modified as shown in equation 2.25. Here a perpetuity consideration is taken in place for any remnants of capacity installed at the end of the time horizon. This is implemented to ensure that the model would not spike the system's capacity near the end of the time horizon due to less relevant present cost values.

$$DF_{d_f} = \frac{1}{(1+r)^{d_f}} + \frac{1}{(1+r)^{d_f+1}} \cdot \frac{1}{\left(1 - \frac{1}{(1+r)}\right)} \tag{2.25}$$

2.3. Objective function development

2.3.1. Resilience in this context

In this study, a system will be considered operationally resilient if it has sufficient autonomy to withstand non-catastrophic unfortunate events. Such events are variations of RE sources and internal plant losses. Due to the many interpretations of the resilient concept in literature, a different epithet is used. This study will refer to the term heteronomy, defined as the lack of autonomy of a system due to its dependence on non-manageable conditions.

2.3.2. Indicator constituents

As indicated in section 2.3.1, the proposed objective function must characterize a system's heteronomy, equivalent to a lack of autonomy. In this study, we consider two essential distinctions of unfortunate events that an autonomous system must endure: external events associated with the intrinsic unpredictable behavior that REs have and its effect on the operation of a plant designed through statistical averages of representative days; and internal events, specific failures in the plant normal operations and its corresponding decrease in production. Both of these events could be interpreted as stochastic. However, this study aims to capture these incidental effects without leaving a deterministic programming approach, striving for simplicity and a reasonable computation time.

2.3.3. External variability

The model must acknowledge the fact that the parameters of solar radiation and wind speed used for the sizing of renewable sources are averages, and for each hour in a representative day there is a historical variance present. In this sense, some locations with a favorable average solar radiation or wind speed might have a high variance, which is not a desired attribute for an off-grid hydrogen plant.

To consider this possible variance, the sizing equations (2.1,2.2) for the renewable sources are used in conjunction with the standard deviation for solar radiation and wind speed to give an estimation of the possible variability in the energy output. This variability is dependent on the installed area of renewable sources at each location, the day and hour of said day (see equations 2.26 and 2.27).

$$\dot{Var}_{PV,t,d,r} = \eta_{PV} \cdot {A^{PV}}_{d,r} \cdot \sigma_{PV,t,d,r} \tag{2.26}$$

$$\dot{Var}_{Wind,t,d,r} = \frac{1}{2} \cdot Cp_{Wind} \cdot {A^{Wind}}_{d,r} \cdot \rho_{Air} \cdot (\sigma_{Wind,t,d,r})^3 \tag{2.27}$$

Where $\sigma_{PV,t,d,r}$ and $\sigma_{Wind,t,d,r}$ correspond to the historical deviation of solar radiation and wind speed in an hourly basis for each trimester and each location. The overall variability will be the sum of both sources. Defined as shown in equation 2.28

$${}^{ext}\delta E^{-}_{t,d,r} = \sum_{e \in RE} \cdot \dot{Var}_{e,t,d,r} \tag{2.28}$$

The system can compensate for this variability with storage. A lack of energy from renewable sources is ultimately perceived as a lack of hydrogen production since not all the necessary power will be supplied to the electrolyzer. Because of this, either the battery sys-

tem can supply power or the tank storage supply mass to withstand this deficiency. The availability of storage that can be used is depicted in equation 2.29.

$$Storage_{t,d,r} = \eta_{Discharge} \cdot {Es^{Acc}}_{t,d,r} + \frac{{ms^{Acc}}_{t,d,r}}{\eta_{AE}} \tag{2.29}$$

The net loss due to external variance can be defined as the difference between the expected source-induced variability and the compensation of the storage systems. Equation 2.30 defines said term as:

$${}^{ext}\Delta {E^{-}}_{t,d,r} = {}^{ext}\ {\delta E^{-}}_{t,d,r} - Storage_{t,d,r} \tag{2.30}$$

If the net externally induced variability ${}^{ext}\Delta {E^{-}}_{t,d,r}$ is greater than zero, the system does not have sufficient storage to withstand the variance that the renewable sources provide.

2.3.4. Internal variability

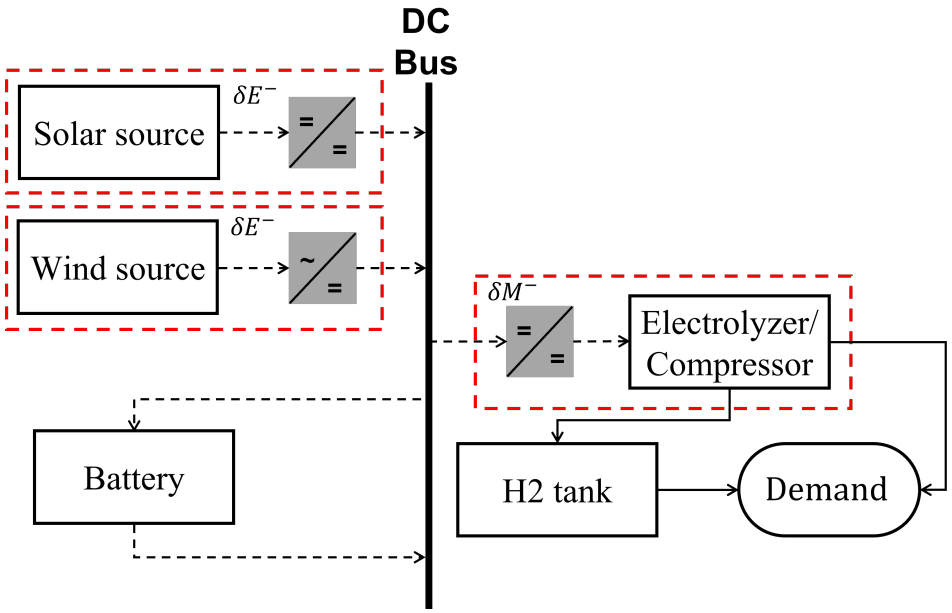

Figure 2.3: Architecture of the hydrogen production plant with relevant converters.

Since unexpected failures in any equipment may occur, plant operation does not work at 100 % of the designed capacity. According to industrial experience, one of the most sensitive pieces of equipment prone to fail in a power system are converters, including DC boosters and rectifiers [53]. Their reliability is heavily dependent on the architecture and control of said component. Figure 2.3 exhibits where said converters are located in the architecture of the plant's electrical system. Internal variability will consider the availability of renewable sources and the electrolyzer based on their associated converters. Since the availability parameter will vary with the converters circuit architecture [53], this study will refer to accepted literature values for solar PV panels and wind turbines of 96 % [54]. DC boosters for alkaline electrolysis circuit designs are still being developed [55], and a 90 % availability is assumed.

As depicted in Figure 2.3, failure in renewable sources will provide a lack of energy (δE^-). Meanwhile, failure in the electrolyzer will have a lack of mass associated (δM^-). Equations

2.31 and 2.32 characterize said energy and mass lack respectively as:

$$^{int}\delta E^{-}{}_{d,r} = \sum_{e \in RE} (1 - \Lambda_e) \cdot Cap_{e,d,r} \tag{2.31}$$

$$^{int}\delta M^{-}{}_{d,r} = (1 - \Lambda_{AE}) \cdot Cap_{AE,d,r} \tag{2.32}$$

As stated in section 2.3.3, the storage system compensates for said variability. In this case, the battery system can compensate for the renewable sources diminished production and mass storage for the electrolyzers. This provides a net internally induced mass and energy variability, which is defined as follows:

$$^{int}\Delta E^{-}{}_{t,d,r} =^{int} \delta E^{-}{}_{d,r} - \eta_{Disch} \cdot Es^{Acc}{}_{t,d,r} \tag{2.33}$$

$$^{int}\Delta M^{-}{}_{t,d,r} =^{int} \delta M^{-}{}_{d,r} - ms^{Acc}{}_{t,d,r} \tag{2.34}$$

2.3.5. Proposed objective

Coupling the externally and internally induced net variability of mass and energy defined in sections 2.3.3 and 2.3.4, the objective function of minimizing the net variability in the system can be defined through equation 2.35.

$$Min \sum_{t,d,r} \eta_{AE} \cdot (^{int}\Delta E^{-}{}_{t,d,r} +^{ext} \Delta E^{-}{}_{t,d,r}) +^{int} \Delta M^{-}{}_{t,d,r} \tag{2.35}$$

This expression can be interpreted as the systems heteronomy since its value will determine if the design can overcome the external and internal variance with the storage systems capacity. A negative value indicates that storage is more than sufficient; a positive value stipulates that storage is insufficient. In this sense, an optimal system can be defined as one with minimal heteronomy.

Chapter 3

Case study

3.1. Locations and climate data

The main objective of this study is to evaluate a proposed resilience objective function to complement the design of HRES for green hydrogen production. This requires that the geographical location of the model presents a mixture of solar radiation and wind speed available so that the combination of solar and wind sources for a hybrid system is considered. Here 5 locations are chosen based on area and climatic conditions data availability: Negrete, Aguapie, Lavapie, Rumena, and Colhue. The Bio-bio region is chosen since it presents favorable sun radiation and wind speed at the 5 locations mentioned, according to the data provided by the national wind [56] and solar observatories [57]. Figure 3.1 provides an overview of the behavior of solar radiation and wind speed in each location, extracted from the used data that considers the historical hourly profiles as well.

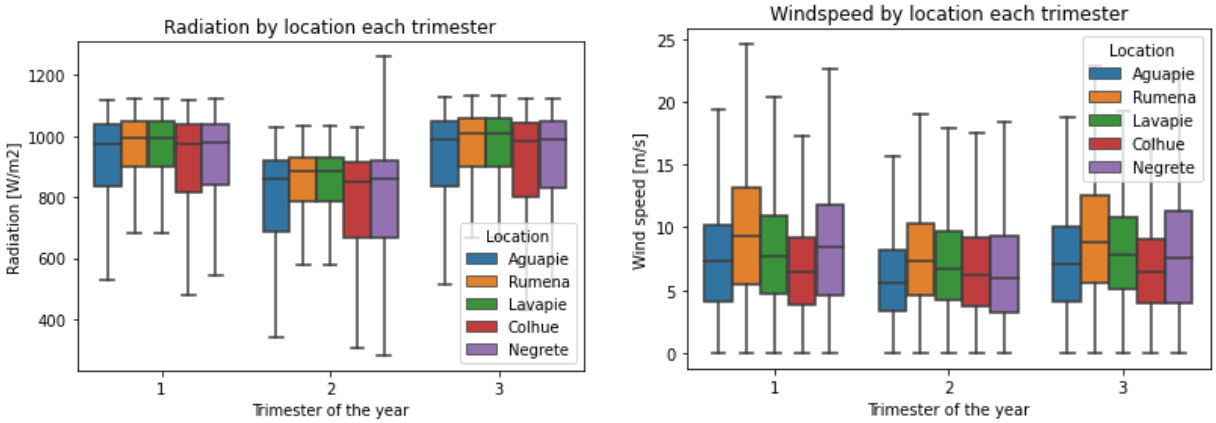

(a) Solar radiation as 3 representative days.

(b) Wind speed as 3 representative days.

Figure 3.1: Averages climate statistics of solar radiation (a) and wind speed (b) for each location at each trimester. (Own elaboration with the data provided by the wind and solar explorers [56, 57])

3.2. Projected demand

Hydrogen is a developing market, and because of this, a forecasting model must be implemented to assess the change in demand through time. Lane et al. (2021) provided a forecast of renewable hydrogen demand at a global scale, implementing a novel method of estimation using Montecarlo simulations to incorporate uncertainty and a learning curve approach considering market growth factor [58]. This study will implement the demand behavior stated by said author, assuming that Chile plans to take 20 % of the demand and the Biobio regions are considered to accomplish 1 % of the total Chilean production for the case study. Annex B presents the values for the learning curve extracted from Lane et al. [58] and the subsequent demand associated with the case study.

3.3. Results

3.3.1. Computation time

The model for the case study in the previous section was implemented in PyOMO [59, 60] and solved using the Gurobi MILP solver [61]. The model constitutes a total of 82,811 variables, where 2,705 variables are binary, and 80,106 are continuous; related through 50,025 equality and 51,745 inequality constraints. The MIP gap terminal condition is maintained at its default value of 1e-4.

3.3.2. Solution multiplicity

Being a MILP problem, it is possible to achieve the same value of the objective function with different values for the arguments, and due to the MIP gap termination condition, better solutions might be obtained by a more thorough search. To evaluate the optimal design, successive integer cuts were implemented to obtain 3 alternate solutions. Equation 3.1 shows the "No good cut" [62], where the variable $z_{i,d,r}$ represents the expansion ($X_{i,d,r}$) and decrease ($Y_{i,d,r}$) binary choices of section 2.1.8, B and NB are the set of basic and non-basic solutions respectively.

$$\sum_{i,d,r \in NB} z_{i,d,r} + \sum_{i,d,r \in B} (1 - z_{i,d,r}) \geq 1 \tag{3.1}$$

Table 3.1: Optimal value for the objective functions in each single-objective model. Alternate solutions' values are presented as a difference from the optimal solution objective.

	Model	
Solution	Economic [USD]	Heteronomic [kg]
Optimal value	1.5996 E+9	-9.4439 E+9
Objective value difference		
Alternative #1	0	+2.61 E+3
Alternative #2	0	-2.31 E+4
Alternative #3	4510	-2.10 E+4

Table 3.1 shows the results for the single-objective models, i.e., those solutions in which the weights for combining the economic and heteronomy objective functions were either zero (purely resilient objective) or one (purely economic objective). The purely economic single-objective model presents 2 alternative solutions with the same value for the objective function. Meanwhile, no equivalent solutions were found for the pure heteronomy single-objective model, but 2 better and 1 worse solutions were found. The difference in the value of the objective functions between the solutions is negligible and the design of the system (i.e. the arguments) does not vary considerably between each solution. As shown in Annex A, only a difference in the stored hydrogen at the end of the time horizon and in some expansion rates is observed. For the rest of the discussion, the results labeled as Optimal value in Table 3.1 are considered.

3.3.3. Pareto front and equilibrium prices

The multi-objective model provides a Pareto front containing all the optimal solutions to the weights considered. An important metric required to asses each Pareto optimal solution is the equilibrium price of hydrogen. This is the price required to achieve a zero Net Present Value (NPV) for the plant investment and production costs. Figure 3.2.a exhibits the Pareto front and the equilibrium price of hydrogen as well.

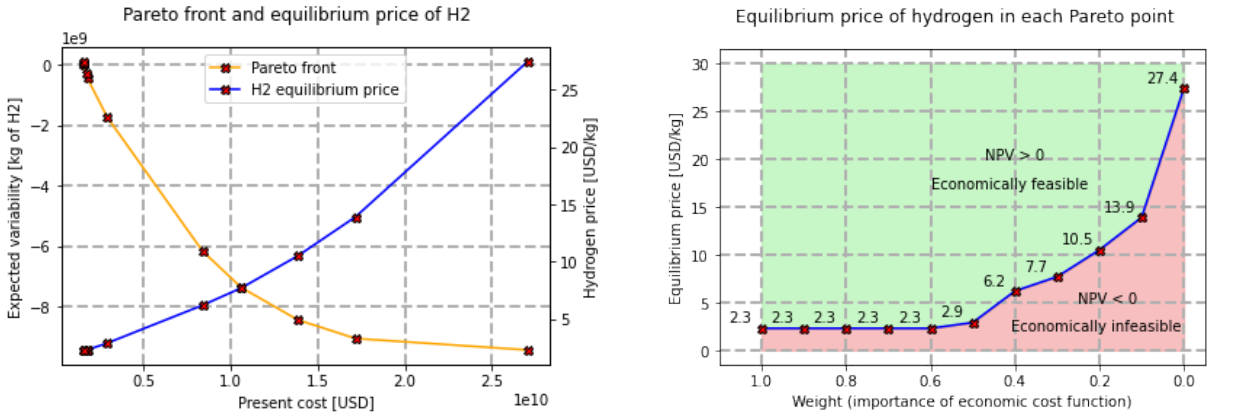

(a) Pareto front and equilibrium price of hydrogen. (b) Hydrogen equilibrium price for each Pareto point.

Figure 3.2: Hydrogen equilibrium price for each Pareto point.

The trade-off between both objective functions relates to the fact that designing a more resilient system requires more investment in storage technologies, directly raising the total cost and the equilibrium price for hydrogen. It is important to note that the heteronomy objective function has, for almost all points, a negative value. This implies that in those solutions the network has enough storage to withstand the expected external and internal losses. Figure 3.2.b shows the equilibrium price for hydrogen vs the weight values for each point in the Pareto curve. The green region above the curve corresponds to the hydrogen prices that provide an economically feasible result (positive NPV). Inversely, the red region corresponds to hydrogen prices that make the system economically unfeasible. A weight of 0.6, associated with a hydrogen equilibrium price of 2.3 $[\frac{\text{USD}}{\text{kgH}_2}]$ is selected as the desired multi-objective solution. This equilibrium price is lower than the 2.6 $[\frac{\text{USD}}{\text{kg}}\text{H}_2]$ benchmark established by the Chilean national hydrogen plan for the Biobio region [63], in addition to presenting a negative heteronomy value. A similar analysis for other weights could be performed if desired.

3.3.4. Capacity expansion: single and multi objective comparison

In this section the different system designs are compared for the single and multi objective models. The capacities of each technology are analyzed for the locations of Negrete and Aguapie, exposing the effects of the proposed heteronomy objective function in the design of the system.

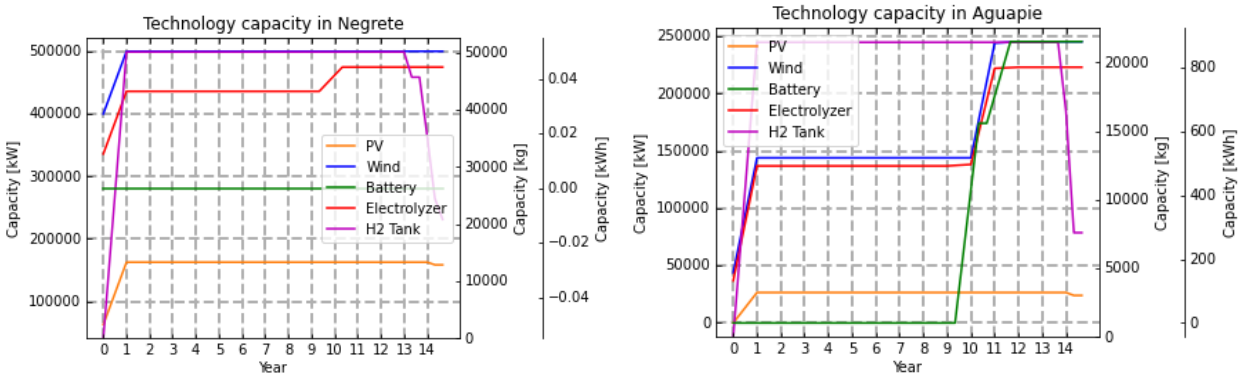

(a) Negrete economic expansion profile

(b) Aguapie economic expansion profile

Figure 3.3: Expansion profiles of the economic model for Negrete (a) and Aguapie (b) respectively.

Figure 3.3 shows the expansion profiles for the economic single objective model in Negrete and Aguapie respectively. Both locations consider hydrogen storage and a hybrid power system of solar and wind for the complete time horizon, where wind is the dominant energy source. In Negrete the installation of energy sources and mass storage is completed by the first year, and an expansion of the electrolyzer capacity is implemented in the 9th year of operation. Meanwhile, Aguapie completes the installation of hydrogen mass storage and solar energy source in the first year of implementation, and an expansion between the 9th and 11th year for the wind source, electrolyzer, and battery system is considered.

Neither location considers a battery system for the first 9 years of operation, and Negrete does not implement a battery system at all. The preference for a hydrogen storage system is related to the more cost/efficient hydrogen mass storage over the lithium-ion batteries for long time periods since the latter have passive losses and present a higher maintenance cost. Because of this, mass storage is preferred over energy storage even when an opportunity cost for hydrogen is implemented.

In both locations a decrease in the hydrogen storage capacity starts from the 13th year until the end of the time horizon to avoid the perpetuity cost effects (see section 2.2.5), where it is cheaper to diminish hydrogen storage and fulfill demand with production and dispatch the already available stored hydrogen.

Figure 3.4 shows the expansion profiles for the heteronomy single objective model in Negrete and Aguapie respectively. Both locations present similar profiles, with the installation of both mass and energy storage systems at maximum capacity for the complete time horizon. a hybrid power system dominated by wind energy is present for each location as well, with a decreasing capacity of the RE sources and electrolyzer until the 3rd and 4th year, when a subsequent expansion is implemented.

The maximization of the storage technologies is associated with the objective function formulation in section 2.3.5, more storage of mass and energy implies a lesser dependence on

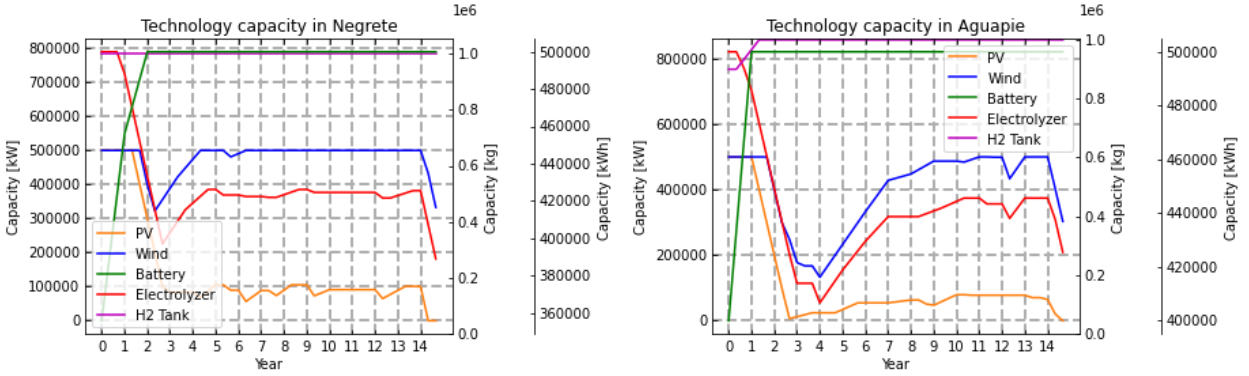

(a) Negrete heteronomy expansion profile

(b) Aguapie heteronomy expansion profile

Figure 3.4: Expansion profiles of the heteronomy model for Negrete (a) and Aguapie (b) respectively.

external and internal variability. The decreasing capacity in the RE sources and electrolyzer technology is related to minimizing the variability of the system (as defined in sections 2.3.3 and 2.3.4), since a bigger installed capacity implies higher internal and external expected variability. Therefore, the heteronomy model tends to maximize storage capacity while maintaining a minimum required energy source and electrolyzer capacity.

Figure 3.5 shows the expansion profiles for the multi objective model. A wind-dominated hybrid power system with dual storage technologies is implemented in both locations. In Negrete, the installation of the power sources, the battery system, and the hydrogen storage are complete in the first year. Aguapie's battery system, hydrogen mass storage, and solar source are fully implemented by the first year, whereas wind power and the electrolyzer have an expansion in the 9th year of operation. Both locations have a decrease in capacity in the last 2 years of the time horizon, associated with the perpetuity effects of the economic objective function. It is important to note that wind turbine capacity in Negrete reached the upper bound established by the Big-M constraint; this could imply that, if technically feasible, a more prominent wind energy source could be preferred at said location.

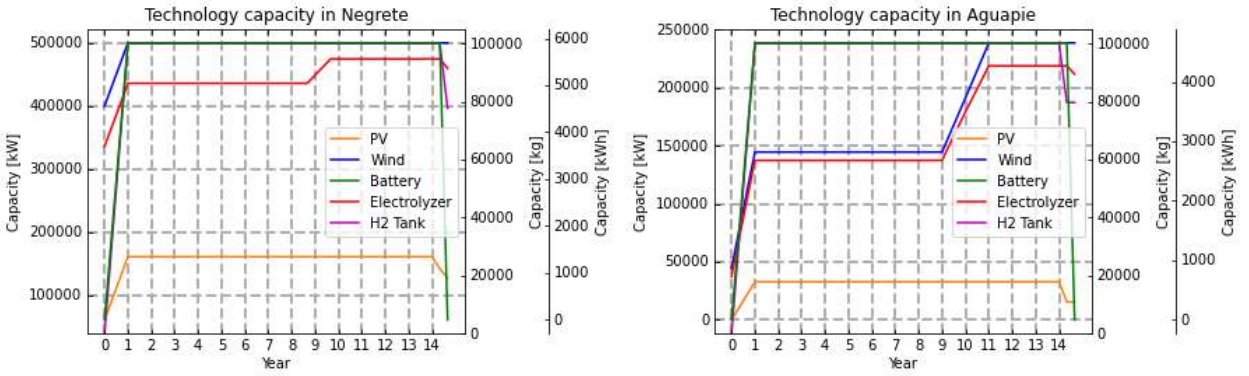

(a) Negrete multi objective expansion profile

(b) Aguapie multi objective expansion profile

Figure 3.5: Expansion profiles of the multi objective model for Negrete (a) and Aguapie (b) respectively.

As exposed in the expansion profiles, the addition of the heteronomy function in a multi objective approach impacts the system design, promoting dual storage throughout the complete time horizon as the key difference to the economic model. In addition, the magnitude of the storage technologies and the power sources also vary. Hydrogen storage increased its maximum value from 50 [ton] in the economic model to 100 [ton] in the multi objective model in Negrete, and 21 [ton] to 100 [ton] in Aguapie. Energy storage also increased compared to the economic model, from 800 [kWh] to 4,600 [kWh] in Aguapie, and from 0 [kWh] to 5,900 [kWh] in Negrete. A slight increase in solar power capacity is also perceived in Aguapie.

3.3.5. The role of storage: Single and multi objective comparison

Here, the use of storage and its effects on the system design are discussed in relation to the capacity expansion profiles and the proposed heteronomy objective function behavior. Figure 3.6 shows the mass stored in each location through the years for the economic, heteronomy, and multi objective models respectively.

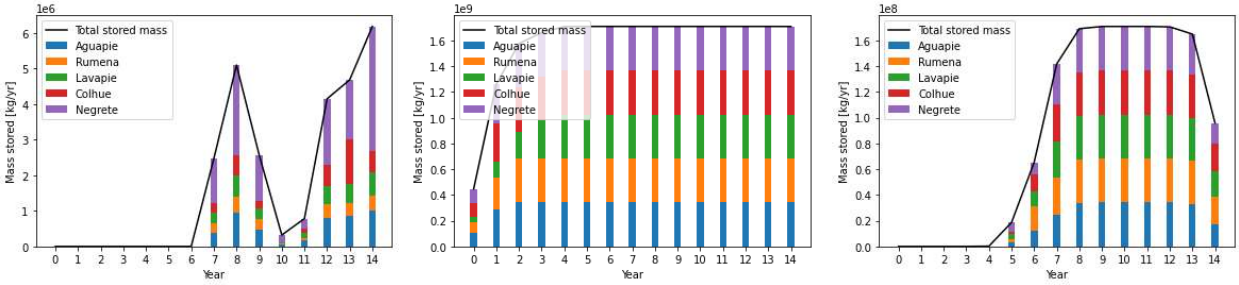

(a) Economic model. (b) Heteronomy model. (c) Multi objective model.

Figure 3.6: Mass storage per location profile for the single and multi objective models.

As seen in Figure 3.6, the economic model has a null storage of H_2 mass the first six years, presenting peaks before and after the 10 years of operation. The first peak (8th year) is related to the capacity expansion profiles present in Figures 3.3.a and 3.3.b. The 10th year of the horizon is when most of the system increases its capacity, and since this requires a year to accomplish, the network must have enough storage to fulfill the increase in demand associated with that year beforehand. The second peak after the 10th year relates to the end-of-time effects in the economic objective function since the system stores hydrogen mass to fulfill demand at the closing year of operation. The heteronomy model increases storage rapidly reaching a constant value by the 3rd year (see Figure 3.6.b), since the purely heteronomy-based model prefers to maximize storage as mentioned in section 3.3.4. The multi-objective model encompasses characteristics of the heteronomy model conservatively, increasing the stored mass by the 3rd year of implementation with a less steep tendency.

The effects of these different storage profiles can be addressed through the heteronomy objective function value since it measures how much autonomy the designed system has. Figure 3.7 exhibits the heteronomy of the single and multi-objective models respectively for Aguapie.

Figure 3.7.a shows that the total heteronomy value of the economic model design is positive throughout the complete time horizon. This is evidence that the designed system is lacking autonomy and that it would be vulnerable in front of the exogenous variability of RE sources and the endogenous component failure. Hence, the use of storage in the economic model is

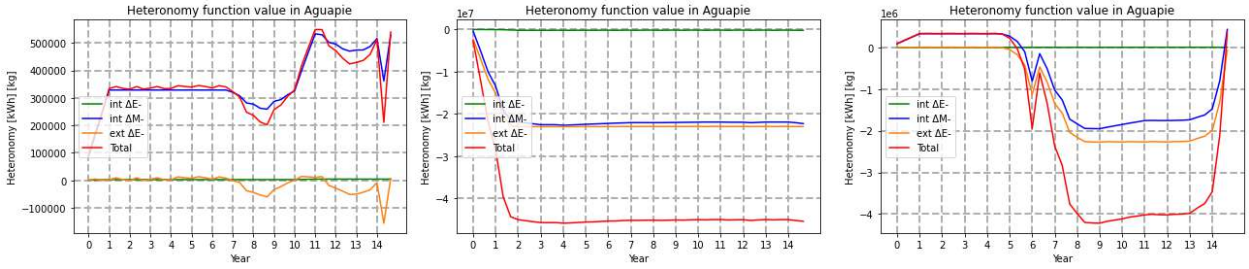

(a) Economic model. (b) Heteronomy model. (c) Multi objective model.

Figure 3.7: Heteronomy objective function behavior.

instrumental to the expansion and closing of the system and not to the operational resilience of the design. Meanwhile, the heteronomy model has a negative heteronomy value for the complete time horizon, over-compensating for the exogenous and endogenous effects. The multi objective model presents a positive value of heteronomy for the first 5 years, reaching a negative value for the rest of the evaluated horizon. This indicates that the multi objective approach manages to design the storage capacity of the system as a way to improve its performance in the face of adversity.

The higher installation of storage capacity discussed in section 2.1.8 and the increase of total stored mass present in this section correlates to the behavior shown in Figure 3.7. The addition of the heteronomy function succeeds in producing a system that manages to be more operationally resilient in front of the considered exogenous and endogenous effects than the purely economic model, without a relevant increase in the hydrogen equilibrium price.

3.3.6. Results remarks

The most relevant results of this study are related to how implementing the proposed objective function complements the design of HRES systems for green hydrogen production. Table 3.2 provides an overview of some of the changes in said design when the economic model is enhanced with the consideration of heteronomy.

In comparison to the economic model, no relevant changes in the start years of each location are seen, where Negrete and Aguapie start in 2025 and the rest in 2026. Meanwhile, wind sources are implemented at a lower magnitude in Lavapie, Aguapie, and Colhue, followed by an increase in solar capacity for said locations. The multi-objective model opts for a hybrid power system, relegating some power capacity from turbines to solar panels. Battery storage has no capacity installed at Negrete and Colhue when only the economic function is considered; in contrast, the multi objective model increases the energy storage capacity of each location. Mass storage also follows the tendency of higher capacities when the heteronomy of the system is considered, increasing to 100 [ton] at each location. The implementation of storage technologies and varied source capacities in the multi-objective approach comes without a noticeable increase in the equilibrium price of hydrogen, and for the selected Pareto solution an investment of 0.37 [USD] is required per kg of H2 mass variability reduction. It is important to note that the shown values consider H_2 opportunity cost, discount factor, and perpetuity effects, which influence the equilibrium price reported.

Figure 3.2.a shows that each Pareto point has more than enough mass and energy storage to withstand the accounted systems variance and that the spike in cost is associated with said increase in storage capacity. Diminishing the value of the big M parameter in the constraint

Table 3.2: Results overview for the economic and MO models. Capacities are presented as intervals of the minimal and maximum values in the time horizon, expresses as [Min - Max].

Result	Model	Rumena	Negrete	Aguapie	Lavapie	Colhue
Starting year	Economic:	2026	2025	2025	2026	2026
	Multi-objective:	2026	2025	2025	2026	2026
Solar source capacity [MW]	Economic:	[0 - 14]	[63 - 162]	[0 - 26]	[0 - 22]	[0 - 25]
	Multi-objective:	[0 - 16]	[61 - 161]	[0 - 32]	[0 - 24]	[0 - 27]
Wind source capacity [MW]	Economic:	[0 - 109]	[400 - 500]	[44 - 245]	[0 - 167]	[0 - 205]
	Multi-objective:	[0 - 109]	[400 - 500]	[44 - 239]	[0 - 161]	[0 - 100]
Battery capacity [MWh]	Economic:	[0 - 2.1]	0	[0 - 0.8]	[0 - 4.4]	0
	Multi-objective:	[0 - 5.3]	[0 - 5.9]	[0 - 4.6]	[0 - 7.7]	[0 - 0.7]
Tank capacity [ton]	Economic:	[0 - 10]	[0 - 50]	[0 - 21]	[0 - 14]	[0 - 16]
	Multi-objective:	[1 - 100]	[0 - 100]	[0 - 100]	[0 - 100]	[0 - 100]
H_2 equilibrium price [USD/kg]		Economic			Multi-objective	
		$ 2.3			$ 2.3	

associated with storage technologies capacity, specifically mass storage, provides a system design with less idle storage, reducing the overall cost of each point in the Pareto frontier and managing a less considerable increase in cost compared to the economic model. The effect of a 75 % reduction in the M constant is depicted by Figure 3.8.

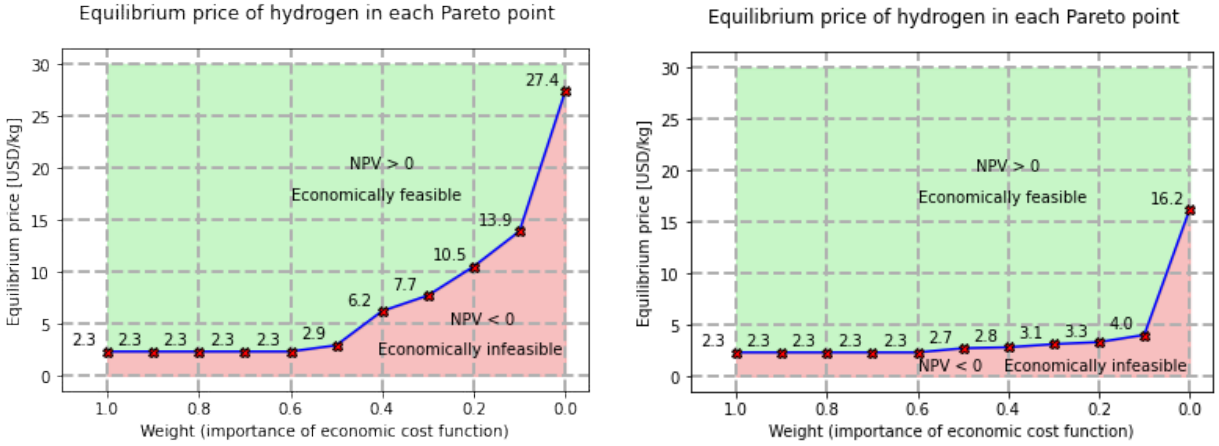

(a) Mass storage M = 10^6

(b) Mass storage M = $2.5 \cdot 10^5$

Figure 3.8: Equilibrium price of hydrogen in each Pareto optimal solution.

The reduction provided a greater economically feasible region due to the lower prices in the Pareto frontier. In consequence, said parameter must be chosen carefully to avoid overestimating the maximum storage capacity of the desired system.

Chapter 4

Conclusion

4.1. Summary of the Thesis and Key Contributions

A deterministic multi-objective mixed integer linear programming model was developed as a decision-making tool to analyze green hydrogen production at a regional scale in Chile. The proposed model considered a novel resilience objective function that encompasses how the designed storage system is capable of mitigating the fluctuations of produced mass and energy due to the intrinsic renewable energy sources uncertainty and probable internal plant failures without leaving a deterministic programming approach, striving for simplicity and reasonable computational resources use.

The proposed objective function complements an economical design incorporating storage technologies with a major capacity that the one in single objective approaches, covering the estimated deficit of mass and energy with sufficient surplus throughout the entire time horizon with a cost of H2 mass variability reduction of 0.37 $[\frac{\text{USD}}{\text{kg H}_2}]$. The mass surplus in storage ought to be considered more than necessary by some investors or decision makers, to which case is necessary to redefine the big M constraint associated with the system's capacity for more conservative mass storage, reducing the overall cost of the system. The hydrogen equilibrium price for both the economic and multi objective model is 2.3 [USD/kg], lower than the 2.6 [USD/kg] estimated by the Chilean hydrogen strategy.

4.2. Future Recommendations

A multi-stage stochastic programming approach could be incorporated to account for the equipment failure in a more rigorous manner. Instead of a decreasing capacity factor, each specific system failure can be taken into consideration simultaneously. It is key to note that said approach would be computationally expensive, where each component failure must be modeled in every location, at every hour, and on any day.

This study's approach can be implemented in large-scale system designs for power-to-H2 and other power-to-X technologies for a more diverse regional design, considering the power system's storage/cost trade-off in a manageable manner. The analysis of a national green hydrogen production architecture can be designed through this thesis methodology. However, due to the size of the problem decomposition strategies would be required.

BIBLIOGRAPHY

[1] Olabi, A. y Abdelkareem, M. A., "Renewable energy and climate change," Renewable and Sustainable Energy Reviews, vol. 158, p. 112111, 2022, doi:10.1016/j.rser.2022.112111.

[2] Maradin, D., "Advantages and disadvantages of renewable energy sources utilization," International Journal of Energy Economics and Policy, vol. 11, pp. 176–183, 2021, doi:10.32479/ijeep.11027.

[3] Swati Negi, L. M., "Hybrid renewable energy system: A review," International Journal of Electronic and Electrical Engineering, 2014.

[4] Kombargi, D. R., Elborai, D. S., Anouti, D. Y., y Hage, R., "The dawn of green hydrogen," strategy, 2021. Revista con proyecciones del mercado de hidrógeno e introducción a su producción.

[5] Ministerio de Ciencia, T. C. e. I., The Chilean Potential for Exporting Renewable Energy. 2021.

[6] Hammer, L. y Veith, E., "Hybrid renewable energy system optimization is lacking consideration of system resilience and robustness: An overview," en ENERGY 2021, The Eleventh International Conference on Smart Grids, Green Communications and IT Energy-aware Technologies, 2021.

[7] Siddaiah, R. y Saini, R., "A review on planning, configurations, modeling and optimization techniques of hybrid renewable energy systems for off grid applications," Renewable and Sustainable Energy Reviews, vol. 58, pp. 376–396, 2016, doi:10.1016/j.rser.2015.12.281.

[8] Ferrer-Martí, L., Domenech, B., García-Villoria, A., y Pastor, R., "A MILP model to design hybrid wind–photovoltaic isolated rural electrification projects in developing countries," European Journal of Operational Research, vol. 226, pp. 293–300, 2013, doi:10.1016/j.ejor.2012.11.018.

[9] Ahadi, A., Kang, S.-K., y Lee, J.-H., "A novel approach for optimal combinations of wind, PV, and energy storage system in diesel-free isolated communities," Applied Energy, vol. 170, pp. 101–115, 2016, doi:10.1016/j.apenergy.2016.02.110.

[10] Lara, C. L., Mallapragada, D. S., Papageorgiou, D. J., Venkatesh, A., y Grossmann, I. E., "Deterministic electric power infrastructure planning: Mixed-integer programming model and nested decomposition algorithm," European Journal of Operational Research, vol. 271, pp. 1037–1054, 2018, doi:10.1016/j.ejor.2018.05.039.

[11] Yu, J., Ryu, J.-H., y beum Lee, I., "A stochastic optimization approach to the design and operation planning of a hybrid renewable energy system," Applied Energy, vol. 247,

pp. 212–220, 2019, doi:10.1016/j.apenergy.2019.03.207.

[12] Alberizzi, J. C., Rossi, M., y Renzi, M., "A MILP algorithm for the optimal sizing of an off-grid hybrid renewable energy system in south tyrol," Energy Reports, vol. 6, pp. 21–26, 2020, doi:10.1016/j.egyr.2019.08.012.

[13] Vera, G., "Development of a method for planning a resilient multi.vector energy system through a multi-objective optimization model," 2020.

[14] Pan, G., Gu, W., Qiu, H., Lu, Y., Zhou, S., y Wu, Z., "Bi-level mixed-integer planning for electricity-hydrogen integrated energy system considering levelized cost of hydrogen," Applied Energy, vol. 270, p. 115176, 2020, doi:10.1016/j.apenergy.2020.115176.

[15] Lim, J. Y., How, B. S., Rhee, G., Hwangbo, S., y Yoo, C. K., "Transitioning of localized renewable energy system towards sustainable hydrogen development planning: P-graph approach," Applied Energy, vol. 263, p. 114635, 2020, doi:10.1016/j.apenergy.2020.114635.

[16] Weimann, L., Gabrielli, P., Boldrini, A., Kramer, G. J., y Gazzani, M., "Optimal hydrogen production in a wind-dominated zero-emission energy system," Advances in Applied Energy, vol. 3, p. 100032, 2021, doi:10.1016/j.adapen.2021.100032.

[17] Corengia, M. y Torres, A. I., "Coupling time varying power sources to production of green-hydrogen: A superstructure based approach for technology selection and optimal design," Chemical Engineering Research and Design, vol. 183, pp. 235–249, 2022, doi:10.1016/j.cherd.2022.05.007.

[18] Li, C., Conejo, A. J., Liu, P., Omell, B. P., Siirola, J. D., y Grossmann, I. E., "Mixed-integer linear programming models and algorithms for generation and transmission expansion planning of power systems," European Journal of Operational Research, vol. 297, pp. 1071–1082, 2022, doi:10.1016/j.ejor.2021.06.024.

[19] Ashok, S., "Optimised model for community-based hybrid energy system," Renewable Energy, vol. 32, pp. 1155–1164, 2007, doi:10.1016/j.renene.2006.04.008.

[20] Obaro, A. Z., Munda, J. L., y Siti, M. W., "Optimal energy management of an autonomous hybrid energy system," en 2018 IEEE 7th International Conference on Power and Energy (PECon), IEEE, 2018, doi:10.1109/pecon.2018.8684131.

[21] Gutiérrez, J. M., Abdul-Jalbar, B., Sicilia, J., y San-José, L. A., "Optimizing a MINLP problem for the grid-connected PV renewable energy consumption under spanish regulations," Computers &amp Industrial Engineering, vol. 168, p. 108109, 2022, doi:10.1016/j.cie.2022.108109.

[22] Ghofrani, M. y Hosseini, N. N., "Optimizing hybrid renewable energy systems: A review," en Sustainable Energy - Technological Issues, Applications and Case Studies, InTech, 2016, doi:10.5772/65971.

[23] Lee, T.-Y. y Chen, C.-L., "Wind-photovoltaic capacity coordination for a time-of-use rate industrial user," IET Renewable Power Generation, vol. 3, no. 2, p. 152, 2009, doi:10.1049/iet-rpg:20070068.

[24] Hakimi, S. y Moghaddas-Tafreshi, S., "Optimal sizing of a stand-alone hybrid power system via particle swarm optimization for kahnouj area in south-east of iran," Renewable Energy, vol. 34, pp. 1855–1862, 2009, doi:10.1016/j.renene.2008.11.022.

[25] Koutroulis, E. y Kolokotsa, D., "Design optimization of desalination systems power-supplied by PV and w/g energy sources," Desalination, vol. 258, pp. 171–181, 2010, doi:10.1016/j.desal.2010.03.018.

[26] Zhao, B., Zhang, X., Chen, J., Wang, C., y Guo, L., "Operation optimization of standalone microgrids considering lifetime characteristics of battery energy storage system," IEEE Transactions on Sustainable Energy, vol. 4, pp. 934–943, 2013, doi:10.1109/tste.2013.2248400.

[27] Fetanat, A. y Khorasaninejad, E., "Size optimization for hybrid photovoltaic–wind energy system using ant colony optimization for continuous domains based integer programming," Applied Soft Computing, vol. 31, pp. 196–209, 2015, doi:10.1016/j.asoc.2015.02.047.

[28] González, A., Riba, J.-R., Rius, A., y Puig, R., "Optimal sizing of a hybrid grid-connected photovoltaic and wind power system," Applied Energy, vol. 154, pp. 752–762, 2015, doi:10.1016/j.apenergy.2015.04.105.

[29] Katsigiannis, Y. A., Georgilakis, P. S., y Karapidakis, E. S., "Hybrid simulated annealing–tabu search method for optimal sizing of autonomous power systems with renewables," IEEE Transactions on Sustainable Energy, vol. 3, pp. 330–338, 2012, doi:10.1109/tste.2012.2184840.

[30] Khatib, T., Mohamed, A., y Sopian, K., "Optimization of a PV/wind micro-grid for rural housing electrification using a hybrid iterative/genetic algorithm: Case study of kuala terengganu, malaysia," Energy and Buildings, vol. 47, pp. 321–331, 2012, doi:10.1016/j.enbuild.2011.12.006.

[31] Sinha, S. y Chandel, S., "Review of recent trends in optimization techniques for solar photovoltaic–wind based hybrid energy systems," Renewable and Sustainable Energy Reviews, vol. 50, pp. 755–769, 2015, doi:10.1016/j.rser.2015.05.040.

[32] Wang, X., Palazoglu, A., y El-Farra, N. H., "Operational optimization and demand response of hybrid renewable energy systems," Applied Energy, vol. 143, pp. 324–335, 2015, doi:10.1016/j.apenergy.2015.01.004.

[33] Kavadias, K., Apostolou, D., y Kaldellis, J., "Modelling and optimisation of a hydrogen-based energy storage system in an autonomous electrical network," Applied Energy, vol. 227, pp. 574–586, 2018, doi:10.1016/j.apenergy.2017.08.050.

[34] Gasser, P., Lustenberger, P., Cinelli, M., Kim, W., Spada, M., Burgherr, P., Hirschberg, S., Stojadinovic, B., y Sun, T. Y., "A review on resilience assessment of energy systems," Sustainable and Resilient Infrastructure, vol. 6, pp. 273–299, 2019, doi:10.1080/23789689.2019.1610600.

[35] Bruneau, M., Chang, S. E., Eguchi, R. T., Lee, G. C., O'Rourke, T. D., Reinhorn, A. M., Shinozuka, M., Tierney, K., Wallace, W. A., y von Winterfeldt, D., "A framework to quantitatively assess and enhance the seismic resilience of communities," Earthquake Spectra, vol. 19, pp. 733–752, 2003, doi:10.1193/1.1623497.

[36] Francis, R. y Bekera, B., "A metric and frameworks for resilience analysis of engineered and infrastructure systems," Reliability Engineering &amp System Safety, vol. 121, pp. 90–103, 2014, doi:10.1016/j.ress.2013.07.004.

[37] Jackson, S. y Ferris, T. L. J., "Resilience principles for engineered systems," Systems

Engineering, vol. 16, pp. 152–164, 2012, doi:10.1002/sys.21228.

[38] Haimes, Y. Y., Crowther, K., y Horowitz, B. M., "Homeland security preparedness: Balancing protection with resilience in emergent systems," Systems Engineering, vol. 11, pp. 287–308, 2008, doi:10.1002/sys.20101.

[39] National Academy of Sciences, Disaster Resilience: A national imperative. The National Academies Press, 2012, doi:10.17226/13457.

[40] Heinimann, H. R. y Hatfield, K., "Infrastructure resilience assessment, management and governance - state and perspectives," en NATO Science for Peace and Security Series C: Environmental Security, pp. 147–187, Springer Netherlands, 2017, doi:10.1007/978-94-024-1123-2_5.

[41] Cho, S., Li, C., y Grossmann, I. E., "Recent advances and challenges in optimization models for expansion planning of power systems and reliability optimization," Computers &amp Chemical Engineering, vol. 165, p. 107924, 2022, doi:10.1016/j.compchemeng.2022.107924.

[42] Nahmmacher, P., Schmid, E., Hirth, L., y Knopf, B., "Carpe diem: A novel approach to select representative days for long-term power system modeling," Energy, vol. 112, pp. 430–442, 2016, doi:10.1016/j.energy.2016.06.081.

[43] Scott, I. J., Carvalho, P. M., Botterud, A., y Silva, C. A., "Clustering representative days for power systems generation expansion planning: Capturing the effects of variable renewables and energy storage," Applied Energy, vol. 253, p. 113603, 2019, doi:10.1016/j.apenergy.2019.113603.

[44] Molina, A. y Martínez, F., "Modelo de generación fotovoltaica," rep. tec., Ministerio de Energía, 2017.

[45] Ackermann, T., ed., Wind Power in Power Systems. John Wiley & Sons, Ltd, 2005, doi:10.1002/0470012684.

[46] Afsharian, S. y Taylor, P. A., "On the potential impact of lake erie wind farms on water temperatures and mixed-layer depths: Some preliminary 1-d modeling using COHERENS," Journal of Geophysical Research: Oceans, vol. 124, pp. 1736–1749, 2019, doi:10.1029/2018jc014577.

[47] Newman, B., "The spacing of wind turbines in large arrays," Energy Conversion, vol. 16, pp. 169–171, 1977, doi:10.1016/0013-7480(77)90024-9.

[48] Schmidt, O., Gambhir, A., Staffell, I., Hawkes, A., Nelson, J., y Few, S., "Future cost and performance of water electrolysis: An expert elicitation study," International Journal of Hydrogen Energy, vol. 42, pp. 30470–30492, 2017, doi:10.1016/j.ijhydene.2017.10.045.

[49] Proost, J., "Critical assessment of the production scale required for fossil parity of green electrolytic hydrogen," International Journal of Hydrogen Energy, vol. 45, pp. 17067–17075, 2020, doi:10.1016/j.ijhydene.2020.04.259.

[50] Martín, M., "Optimal year-round production of DME from CO2 and water using renewable energy," Journal of CO2 Utilization, vol. 13, pp. 105–113, 2016, doi:10.1016/j.jcou.2016.01.003.

[51] El-Sharkh, M., Tanrioven, M., Rahman, A., y Alam, M., "Cost related sensitivity analysis for optimal operation of a grid-parallel PEM fuel cell power plant," Journal of Power

Sources, vol. 161, pp. 1198–1207, 2006, doi:10.1016/j.jpowsour.2006.06.046.

[52] de Impuestos Internos (SII), S., "RevalÚo de sitios no edificados, propiedades abandonadas o pozos lastreros," rep. tec., Servicio de Impuestos Internos, 2021.

[53] Peyghami, S., Wang, Z., y Blaabjerg, F., "A guideline for reliability prediction in power electronic converters," IEEE Transactions on Power Electronics, vol. 35, pp. 10958–10968, 2020, doi:10.1109/tpel.2020.2981933.

[54] Kaviani, A. K., Riahy, G., y Kouhsari, S., "Optimal design of a reliable hydrogen-based stand-alone wind/PV generating system, considering component outages," Renewable Energy, vol. 34, pp. 2380–2390, 2009, doi:10.1016/j.renene.2009.03.020.

[55] Guilbert, D., Collura, S. M., y Scipioni, A., "DC/DC converter topologies for electrolyzers: State-of-the-art and remaining key issues," International Journal of Hydrogen Energy, vol. 42, pp. 23966–23985, 2017, doi:10.1016/j.ijhydene.2017.07.174.

[56] Ministerio de Energía, G. d. C., "Explorador solar." Online, 2023, https://solar.minenergia.cl/inicio.

[57] Ministerio de Energía, G. d. C., "Explorador eólico," 2023, https://eolico.minenergia.cl/inicio.

[58] Lane, B., Reed, J., Shaffer, B., y Samuelsen, S., "Forecasting renewable hydrogen production technology shares under cost uncertainty," International Journal of Hydrogen Energy, vol. 46, pp. 27293–27306, 2021, doi:10.1016/j.ijhydene.2021.06.012.

[59] Bynum, M. L., Hackebeil, G. A., Hart, W. E., Laird, C. D., Nicholson, B. L., Siirola, J. D., Watson, J.-P., y Woodruff, D. L., Pyomo–optimization modeling in python, vol. 67. Springer Science & Business Media, third ed., 2021.

[60] Hart, W. E., Watson, J.-P., y Woodruff, D. L., "Pyomo: modeling and solving mathematical programs in python," Mathematical Programming Computation, vol. 3, no. 3, pp. 219–260, 2011.

[61] Gurobi Optimization, LLC, "Gurobi Optimizer Reference Manual," 2023, https://www.gurobi.com.

[62] Balas, E. y Jeroslow, R., "Canonical cuts on the unit hypercube," SIAM Journal on Applied Mathematics, vol. 23, pp. 61–69, 1972, doi:10.1137/0123007.

[63] Ministerio de Energía, G. d. C., "Estrategia nacional de hidrÓgeno verde," rep. tec., 2020.

[64] F., P., A., B., y C., B., "Thermal management of solid oxide electrolysis cell systems through air flow regulation," Chemical Engineering Transactions, vol. 61, pp. 1069–1074, 2017, doi:10.3303/CET1761176.

[65] Christensen, A., "Assessment of hydrogen production costs from electrolysis: United states and europe," rep. tec., Three Seas Consulting, 2020.

[66] Lorenzo, J., "Rendimiento de placas solares," 2015, <https://www.sfe-solar.com/>.

[67] Pamparana, G., Kracht, W., Haas, J., Díaz-Ferrán, G., Palma-Behnke, R., y Román, R., "Integrating photovoltaic solar energy and a battery energy storage system to operate a semi-autogenous grinding mill," Journal of Cleaner Production, vol. 165, pp. 273–280, 2017, doi:10.1016/j.jclepro.2017.07.110.

[68] Yang, H., Lu, L., y Zhou, W., "A novel optimization sizing model for hybrid solar-wind power generation system," Solar Energy, vol. 81, pp. 76–84, 2007, doi:10.1016/j.solener.2006.06.010.

[69] CNE, "Fijación de presios de nuco corto," rep. tec., Comisión Nacional de Energía, 2022.

[70] LAZARD, "Lazard's levelized cost of energy analysis - version 15.0," 2021, <https://www.lazard.com>.

[71] W, C. y Frazier, A., "Nrel: technical report: Cost projections for utility-scale battery storage," rep. tec., National Renewable Energy Laboratory (NREL), 2019.

[72] Parks, G., Boyd, R., Cornish, J., y Remick, R., "Hydrogen station compression, storage, and dispesing technical status and costs: Systems integration," rep. tec., National Renewable Energy Laboratory (NREL), 2014.

[73] Administration, U. E. I., "Cost and performance characteristics of new generating technologies," rep. tec., U.S. Energy Information Administration, 2021.

[74] Yates, J., Daiyan, R., Patterson, R., Egan, R., Amal, R., Ho-Baille, A., y Chang, N. L., "Techno-economic analysis of hydrogen electrolysis from off-grid stand-alone photovoltaics incorporating uncertainty analysis," Cell Reports Physical Science, vol. 1, p. 100209, 2020, doi:10.1016/j.xcrp.2020.100209.

[75] (NREL), N. R. E. L., "Hydrogen station compression,storage, and dispensingtechnical status and costs," rep. tec., NREL, 2014.

[76] Dursun, B. y Aykut, E., "An investigation on wind/PV/fuel cell/battery hybrid renewable energy system for nursing home in istanbul," Proceedings of the Institution of Mechanical Engineers, Part A: Journal of Power and Energy, vol. 233, pp. 616–625, 2019, doi:10.1177/0957650919840519.

ANNEXES

ANNEX A. Alternative designs

Figure A.1 shows an example of the design variations found through the integer cuts for Aguapie.

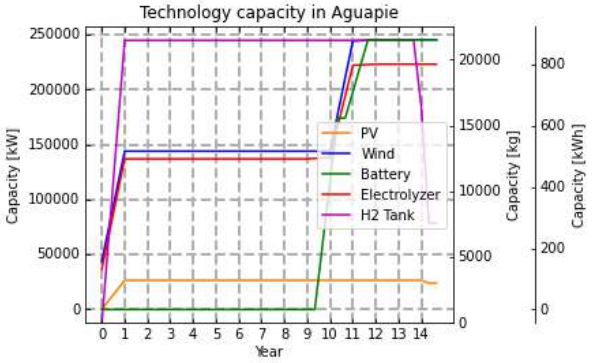

(a) Original expansion profile

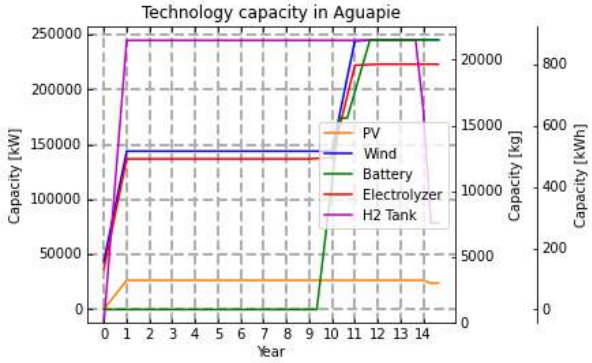

(b) Expansion profile of the first alternative

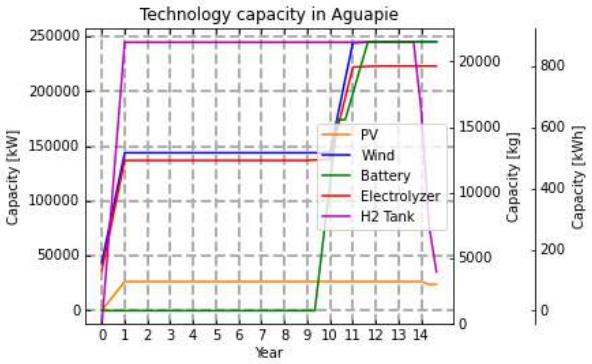

(c) Expansion profile of the second alternative

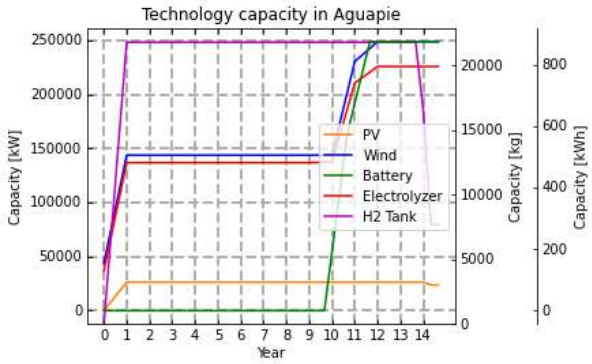

(d) Expansion profile of the third alternative

Figure A.1: Alternative designs for the Aguapie expansion. Obtained through the "No good" integer cut.

Only slight variations of design can be seen for the final hydrogen storage capacity, where the alternative of Figure A.1.c decreases capacity more than the other solutions. Another difference can be seen for the profile of the third alternative design in Figure A.1.d, where the expansion of the 9th year is delayed one trimester, incurring in a step-wise increase before

the maximum capacities for wind turbines, electrolyzer, and battery storage is achieved. None of the found solutions differ from each other considerably, neither in the magnitude of the installed capacities nor in the overall profile for the system expansion.

ANNEX B. Hydrogen demand projection

The global hydrogen demand behavior is modeled as a learning curve according to equation B.1.

$$D_t = \frac{D_f}{1 + e^{-k \cdot (t - t_0)}} + D_0 \tag{B.1}$$

Where D_t is the global hydrogen demand at time t, D_F is the final market production, D_0 is the initial market production, k is the growth factor and t_0 is the initial year of evaluation. It's assumed that Chile aims to reach 20 % of the market share, whereas the Biobio region is contemplated to produce 1 % of the national hydrogen production. Figure B.1 presents the global demand projection in the study's time horizon, where the mean value of demand is used for the Biobio share.

Table B.1: Parameters for the demand projection through a learning curve behavior.

Parameter	Value	Unit	Reference
Initial market	Mean: $1.5 \cdot 10^9$	$[kg/yr]$	[58]
	SD: 0	$[kg/yr]$	
Final market	Mean: $1.66 \cdot 10^{11}$	$[kg/yr]$	[58]
	SD: $2.4 \cdot 10^{10}$	$[kg/yr]$	
Growth	0.1	[-]	[58]
Shift	4.5	[-]	[58]
Biobio global market share	0.1 %	[-]	Assumed

ANNEX C. Electrolysis technologies cost comparison

Schmidt et al. [48] and Proost et al. [49] provide the $\frac{\Delta H}{\eta_{Electr.}}$ parameter for alkaline electrolysis (AE) and proton exchange membrane electrolysis (PEME), meanwhile, Petipas et al. [64] reports the value for solid oxide electrolysis (SOE). The levelized cost of each technology is reported by Christensen [65]. With the levelized cost and efficiency, the cost of mass production can be calculated as depicted in equation C.1.

$$Cost^{Mass}_{Electr.} = C^{Impl}_{Electr.} \cdot \Delta H / \eta_{Electr.} \tag{C.1}$$

Equations C.2, C.3, and C.4 show the cost for each electrolyzer technology.

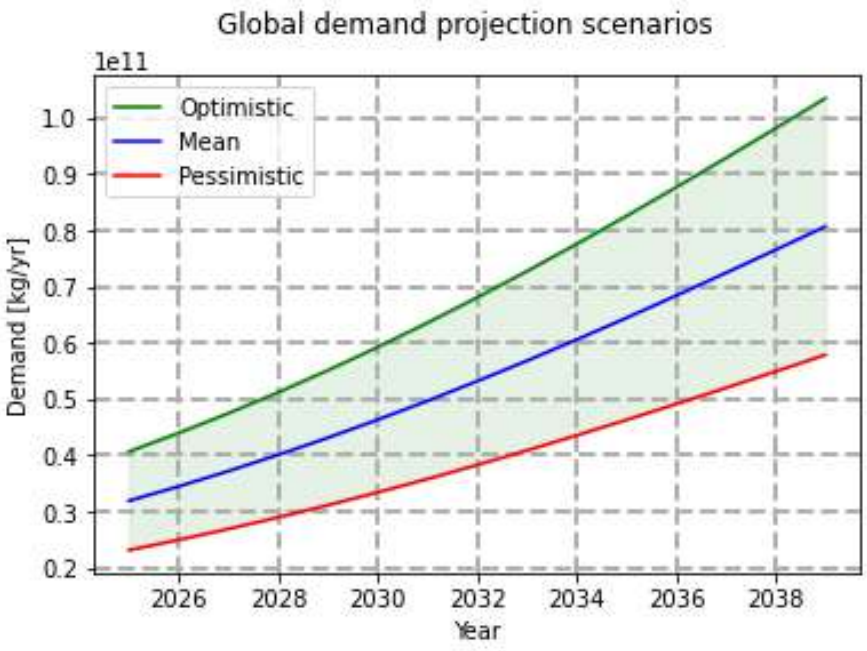

Figure B.1: Global hydrogen demand projection through a learning curve for pessimistic, normal and optimistic scenarios.

$$Cost_{AE}^{Mass} = 1,083 \left[\frac{USD}{kW}\right] \cdot 53.7 \left[\frac{kW}{kg/h}\right]$$
$$\approx 58,157 \left[\frac{USD}{kg/h}\right] \tag{C.2}$$

$$Cost_{PEME}^{Mass} = 1,182 \left[\frac{USD}{kW}\right] \cdot 53.7 \left[\frac{kW}{kg/h}\right]$$
$$\approx 63,473 \left[\frac{USD}{kg/h}\right] \tag{C.3}$$

$$Cost_{SOE}^{Mass} = 2,285 \left[\frac{USD}{kW}\right] \cdot 42.7 \left[\frac{kW}{kg/h}\right]$$
$$\approx 97,570 \left[\frac{USD}{kg/h}\right] \tag{C.4}$$

The AE presents the lower cost of hydrogen production according to the parameters that the formulated model uses. Since no difference in availability can be factually established, the economic part of the multi-objective function will always choose AE technologies over their counterparts.

ANNEX D. Condensed model formulation and nomenclature

1. **Sets**

   - Renewable energy sources:

$$e \in RE = \{PV, Wind\}$$

   - Sized technologies:

$$i \in I = RE \cup \{AE, Compressor, Battery, Tank\}$$

   - Discrete time of day:

$$t \in T = \{0, 1, 2, 3, ..., 23\}$$

   - Representative days (trimester) in a 15 year time horizon:

$$d \in D = \{0, 1, 2, 3, ..., 44\}$$

   - Locations where plants can be installed:

$$r \in R = \{Aguapie, Rumena, Lavapie, Colhue, Negrete\}$$

2. **Variables**

   - If location r is used in the regional production:

$$H_r \in \{0, 1\}$$

   - If technology i starts a expansion project at day d in location r:

$$Y_{i,d,r} \in \{0, 1\}$$

   - If technology i starts a downgrade project at day d in location r:

$$X_{i,d,r} \in \{0, 1\}$$

   - Amount of capacity expansion/downgrade for the project associated with technology i at day d in location r:

$$CapE_{i,d,r} \;\; CapD_{i,d,r} \in \mathbb{R}^+$$

   - Capacity of technology i at day d in location r:

$$Cap_{i,d,r} \in \mathbb{R}^+$$

   - Bough terrain in location r:

$$A_r \in \mathbb{R}^+$$

- Installed area of PV panels and wind turbine swipe area in location r:

$$A^{PV}{}_{d,r}\ A^{Wind}{}_{d,r} \in \mathbb{R}^+$$

- Compressor power consumption in time t at day d in location r:

$$Power^{Comp}{}_{t,d,r} \in \mathbb{R}^+$$

- Energy flow directed to battery storage in time t at day d in location r:

$$\dot{E}_s^{in}{}_{t,d,r} \in \mathbb{R}^+$$

- Energy flow directed to the AE from the battery system in time t at day d in location r:

$$\dot{E}_s^{out}{}_{t,d,r} \in \mathbb{R}^+$$

- Energy flow directed to the AE from the energy source e in time t at day d in location r:

$$\dot{E}_{e,t,d,r}^{Direct} \in \mathbb{R}^+$$

- Energy flow directed to the battery system from the energy source e in time t at day d in location r:

$$\dot{E}_{e,t,d,r}^{Storage} \in \mathbb{R}^+$$

- Energy flow supplied to the AE in time t at day d in location r:

$$\dot{E}_{AE}^{in}{}_{t,d,r} \in \mathbb{R}^+$$

- Mass flow out from the AE in time t at day d in location r:

$$\dot{m}_{t,d,r}^{out} \in \mathbb{R}^+$$

- Mass flow supplied to the hydrogen tank in time t at day d in location r:

$$\dot{m}_s^{in}{}_{t,d,r} \in \mathbb{R}^+$$

- Mass flow supplied to demand directly from the AE in time t at day d in location r:

$$\dot{m}_{t,d,r}^{d} \in \mathbb{R}^+$$

- Mass flow supplied to demand from the hydrogen tank in time t at day d in location r:

$$\dot{m}_s^{out}{}_{t,d,r} \in \mathbb{R}^+$$

- Energy stored in the battery system in time t at day d in location r:

$$E^{Acc}{}_{t,d,r} \in \mathbb{R}^+$$

- Mass stored in the hydrogen tank in time t at day d in location r:

$$m^{Acc}{}_{t,d,r} \in \mathbb{R}^+$$

3. **Constraints**

- If the location isn't chosen, no capacity is allowed:

$$Cap_{i,d,r} \leq M \cdot H_r \tag{D.1}$$

- Expansion and downgrade projects can't start on the same day for technology i at day d in location r:

$$Y_{i,d,r} + X_{i,d,r} \leq 1 \tag{D.2}$$

- Expansion projects last for a year in implementation. Meanwhile, no expansion or downgrade of the same technology can occur:

$$\sum_{\hat{d}=d+1}^{d+2} Y_{i,\hat{d},r} \leq 2 \cdot (1 - Y_{i,d,r}) \tag{D.3}$$

$$\sum_{\hat{d}=d+1}^{d+2} X_{i,\hat{d},r} \leq 2 \cdot (1 - Y_{i,d,r}) \tag{D.4}$$

- The choice of expansion or downgrade bounds the augmentation or diminution of capacity:

$$CapE_{i,d,r} \leq M \cdot Y_{i,d,r} \tag{D.5}$$

$$CapD_{i,d,r} \leq M \cdot X_{i,d,r} \tag{D.6}$$

- Variation of capacity represented as a stock constraint. The implementation of upgrades is achieved progressively through the year by trimester:

$$\begin{aligned} Cap_{i,d,r} = Cap_{i,d-1,r} + \\ \sum_{\hat{d}=d}^{d+2} \left(\frac{1}{3} CapE_{i,\hat{d}} \right) - CapD_{i,d-2,r} \end{aligned} \tag{D.7}$$

- Total produced solar energy depends on installed area:

$$\dot{E}^{Direct}_{PV,t,d,r} + \dot{E}^{Storage}_{PV,t,d,r} = \eta_{PV} \cdot A^{PV}{}_{d,r} \cdot G^{Sun}{}_{t,d,r} \tag{D.8}$$

- Total produced wind energy depends on installed swipe area:

$$\dot{E}^{Direct}_{Wind,t,d,r} + \dot{E}^{Storage}_{Wind,t,d,r} = \frac{1}{2} Cp_{Wind} \cdot {A^{Wind}}_{d,r} \cdot \rho_{Air} \cdot (v_{Windt,d,r})^3 \tag{D.9}$$

- Renewable energy is bounded by installed capacity:

$$\dot{E}^{Direct}_{e,t,d,r} + \dot{E}^{Storage}_{e,t,d,r} \leq Cap_{e,d,r} \tag{D.10}$$

- Installed area of PV and wind cannot exceed bought terrain at each location:

$${A^{PV}}_{d,r} + \frac{{A^{PV}}_{d,r}}{\lambda} \leq A_r \tag{D.11}$$

- Bought terrain cannot exceed the maximum available area:

$$A_r \leq H_r \cdot A^{Max}_r \tag{D.12}$$

- The battery system has to operate in between acceptable SOC values to preserve functionality:

$$SOC_{min} \cdot Cap_{Battery,d,r} \leq {E^{Acc}}_{t,d,r} \tag{D.13}$$

$${E^{Acc}}_{t,d,r} \leq SOC_{max} \cdot Cap_{Battery,d,r} \tag{D.14}$$

- Effective mass flow out of the electrolyzer:

$$\frac{\eta_{AE}}{\Delta H} \cdot \dot{E}^{in}_{AEt,d,r} = \dot{m}^{out}_{t,d,r} \tag{D.15}$$

- Maximum capacity for the electrolyzer:

$$\dot{E}^{in}_{AEt,d,r} \leq Cap_{AE,d,r} \tag{D.16}$$

- Compressors capacity restricts outgoing mass flow:

$$\dot{m}^{d}_{t,d,r} + {\dot{m}^{out}_{s}}_{t,d,r} \leq Cap_{Compressor,d,r} \tag{D.17}$$

- Compressor power consumption according to mass flow:

$$Power^{Comp}_{t,d,r} = k_{Compressor} \cdot \dot{m}^{out}_{AEt,d,r} \tag{D.18}$$

- Mass storage must respect a maximal hydrogen level as a safety measure:

$$0 \leq {ms^{Acc}}_{t,d,r} \leq HTL_{max} \cdot Cap_{Tank,d,r} \tag{D.19}$$

- Energy balance for the battery system:

$${Es^{Acc}}_{t,d,r} = \left[1 - L^{Battery}\right] \cdot {Es^{Acc}}_{t-1,d,r} + \Delta t \cdot \left(\eta_{Charge} \cdot {\dot{Es}^{in}}_{t-1,d,r} - \frac{{\dot{Es}^{out}}_{t-1,d,r}}{\eta_{Discharge}} \right) \tag{D.20}$$

- Energy balance for total energy entering the battery system:

$$\sum_{e \in RE} \dot{E}^{Storage}_{e,t,d,r} = \dot{E}^{\ in}_{st,d,r} \tag{D.21}$$

- Energy balance for total energy entering the electrolyzer:

$$\sum_{e \in RE} \dot{E}^{Direct}_{e,t,d,r} + \dot{E}^{\ in}_{st,d,r} = \dot{E}^{in}_{AEt,d,r} + Power^{Comp}_{t,d,r} \tag{D.22}$$

- Compressor mass balance:

$$\dot{m}^{out}_{AEt,d,r} = \dot{m}^{d}_{t,d,r} + \dot{m}^{\ in}_{s\ t,d,r} \tag{D.23}$$

- Hydrogen storage mass balance:

$$ms^{Acc}{}_{t,d,r} = ms^{Acc}{}_{t-1,d,r} + \Delta t \cdot \left(\dot{m}s^{in}_{t-1,d,r} - \frac{\dot{m}s^{out}_{t-1,d,r}}{\eta_{Tank}} \right) \tag{D.24}$$

- Demand is associated to a complete trimester by the d index. Considering that a trimester contains 120 representative days the demand fulfilment is characterized as:

$$120 \cdot \left(\sum_{t \in T\ r \in R} \dot{m}^{out}_{s\ t,d,r} + \dot{m}^{s}_{t,d,r} \right) = Demand_d \tag{D.25}$$

4. **Objective functions**

- Minimize present cost:

$$\text{Min: } Terrain + \sum_{d \in D} DF_d \cdot (CAPEX_d + OPEX_d + C^{H_2}{}_{Op_d}) \tag{D.26}$$

- Minimize heteronomy:

$$\text{Min: } {}^{int}\Delta M^{-}{}_{t,d,r} + \eta_{AE} \cdot ({}^{int}\Delta E^{-}{}_{t,d,r} + {}^{ext}\ \Delta E^{-}{}_{t,d,r}) \tag{D.27}$$

ANNEX E. Parameter values

Table E.1: Parameters for the case study

Parameter		Value	Unit	Source
$\frac{\Delta H}{\eta_{AE}}$		53.7	[kWh/kg]	[48], [49]
η_{PV}		20 %	[kW_{out}/kW_{in}]	[66]
$\eta_{Charge,\ Disch.,\ Tank}$		95 %	[-]	[67]
λ		$1.7 \cdot 10^{-3}$	[m^2 swipe/m^2 terrain]	[46][47]
C_P^{Wind}		0.4	[-]	[57]
HTL_{Max}		95 %	[-]	Assumed
$k_{Compressor}$		4	[kWh/kg]	[17]
$L^{Battery}$		0.02 %	[-]	[68]
$P_{H_2}^{Sale}$		2.6	[USD/kg]	[63]
Λ_i	PV, Wind	96 %	[-]	[54]
	Electrolyzer	90 %	[-]	Assumed
A_r^{Max}	Aguapie	50.000	[ha]	[52]
	Rumena	2.000	[ha]	[52]
	Lavapie	850	[ha]	[52]
	Colhue	41.200	[ha]	[52]
	Negrete	20.000	[ha]	[52]
C_i^{Impl}	PV	970	[USD/kW]	[69]
	Wind	1.350	[USD/kW]	[70]
	Battery	350	[USD/kWh]	[71]
	AE	1.083	[USD/kW]	[65]
	Compressor	250	[USD/(kg/hr)]	[17]
	Tank	1.000	[USD/kg]	[72]
C_i^{Op} (as trimester)	PV	0.55 %	[-]	[69]
	Wind	0.6 %	[-]	[73]
	Battery	2.5 %	[-]	[73]
	AE	0.6 %	[-]	[74]
	Compressor	0.24 %	[-]	[75]
	Tank	0.24 %	[-]	[76]
M	Upgrade/Downgrade	10^5	[-]	-
	PV,Wind,Battery	10^6	[-]	-
	AE, Compressor, Tank	$5 \cdot 10^5$	[-]	-